INFORMATION TO USERS

This manuscript has been reproduced from the microfilm master. UMI films the text directly from the original or copy submitted. Thus, some thesis and dissertation copies are in typewriter face, while others may be from any type of computer printer.

The quality of this reproduction is dependent upon the quality of the copy submitted. Broken or indistinct print, colored or poor quality illustrations and photographs, print bleedthrough, substandard margins, and improper alignment can adversely affect reproduction.

In the unlikely event that the author did not send UMI a complete manuscript and there are missing pages, these will be noted. Also, if unauthorized copyright material had to be removed, a note will indicate the deletion.

Oversize materials (e.g., maps, drawings, charts) are reproduced by sectioning the original, beginning at the upper left-hand corner and continuing from left to right in equal sections with small overlaps. Each original is also photographed in one exposure and is included in reduced form at the back of the book.

Photographs included in the original manuscript have been reproduced xerographically in this copy. Higher quality 6" x 9" black and white photographic prints are available for any photographs or illustrations appearing in this copy for an additional charge. Contact UMI directly to order.

UMI®

Bell & Howell Information and Learning
300 North Zeeb Road, Ann Arbor, MI 48106-1346 USA
800-521-0600

Stabilization of Transition States of Organic Reactions by Cyclodextrins, Micelles, and Dendrimers.

Alexei A. Fedortchenko

A Thesis
in
the Department
of
Chemistry and Biochemistry

Presented in Partial Fulfilment of the Requirements
for the Degree of Master of Science
at Concordia University
Montreal, Quebec, Canada
December, 1997

Abstract.

Stabilization of Transition States of Organic Reactions by Cyclodextrins, Micelles, and Dendrimers.

Alexei Fedortchenko.

Micelles of cetyltrimethylammonium bromide (CTAB) catalyze the basic cleavage of *p*-nitrophenyl alkanoates, whereas micelles of sodium dodecyl sulphate (SDS) inhibit this reaction. The strength of binding of the esters to both CTAB and SDS shows the same linear dependence and sensitivity to the acyl chain length, but the catalysis by CTAB and the inhibition by SDS do not depend on this parameter.

Micelles of SDS catalyze the hydrolysis of aromatic acetals and orthoesters in the acidic solution. There is no sharp linear correlation between the substrate and the transition state binding for different acetals and orthoesters, which reflects the importance of both nature of the substituent, and its location in the molecule of the substrate.

Amino- and carboxylate-terminated dendrimers modestly catalyze the basic cleavage of *p*-nitrophenyl alkanoates. Both substrate and transition state binding are independent on the ester acyl chain length, but were found to be a function of the dendrimer generation number. Carboxylate-terminated dendrimers catalyze the hydrolysis of aromatic acetals and orthoesters in the acidic solution. The observed dependence of the substrate and the transition state binding on the nature of the substituent supported the previously made suggestion that the interior of PAMAM dendrimers possesses hydrophilic character.

The hydrolysis of aromatic acetals and orthoesters is retarded by cyclodextrins. The magnitude of the effect depends on the size of cyclodextrin cavity. The observed rate retardation is attributed to the unfavourable transition state binding to cyclodextrins, and possible retardation of diffusional separation of carboxonium ion and the newly formed alcohol molecule.

Acknowledgments.

I would like to thank Prof. Oswald S. Tee for being my research supervisor and for his constant support throughout my stay in Concordia.

I also would like to thank:

Concordia University for financial support.

Prof. Jack, Prof. Baldwin, Prof. Kornblatt and Prof. Colebrook for being members of my committee.

Dr. Gadosy for his help and advice during my first months in the lab.

Mrs. Carole Coutts.

Michael Boyd for the help with running NMR spectra.

Students of our lab- Isabelle, Paul, and Samer.

Table of Contents.

List of Figures.

List of Tables.

List of Abbreviations.

ADMA	acetophenone dimethyl acetal
BDMA	benzaldehyde dimethyl acetal
BDEA	benzaldehyde diethyl acetal
CD	cyclodextrin
CMDP	critical molecular design parameter
CTAB	cetyltrimethylammonium bromide
D n	dendrimer of the generation n
pNPAlk	*p*-nitrophenyl alkanoate
SDS	sodium dodecyl sulphate
TMOB	trimethyl orthobenzoate
TS	transition state

Introduction.

Nanoscale structures are not alien to Nature. Just recall enzymes, and the importance of the nanouniverse for life becomes evident. Besides, the idea of using naturally occurring, and, to the greater extent, artificially created nanoscopic devices in engineering and electronics looks extremely attractive[1]. Self-organization, self-assembly, self-control of critical molecular design parameters (CMDPs)[1,2] lay the foundation of nanochemistry, which is a subject of field of science known as supramolecular chemistry, meaning chemistry "beyond the molecule."[2] Hydrophobic, Van der Waals, electrostatic, and other non-covalent interactions are common forces by which supermolecules undergo self-assembly [2,3]. Recent advances in synthetic and polymer chemistry, however, have given a new look to supramolecular chemistry with dendrimers, which are covalently bonded mimics of supermolecules. In the course of the present work properties of three different supramolecular systems have been studied: micelles (self-assembling molecular aggregates), dendrimers (synthetically designed molecules, that often referred to as "building blocks for a nanoscopic chemistry set"[4]), and cyclodextrins (cyclic oligosaccharides). The main point of interest was to study the stabilization of the transition state (TS) of some organic reactions by these molecular assemblies. While cyclodextrins have received extensive investigation from the point of view of TS stabilization[5-8], micelles and dendrimers were examined in this manner for the first time.

Surfactants.

Micelles are build up from molecules known as surfactants. Surfactants are substances that alter the surface or interfacial free energies by absorbing onto the surfaces or interfaces of the system they are present in[9,10]. The word "surfactant" itself stands for "surface-active agent." Surfactants possess a large variety of structural features, but all of them must have one dominant property: they are amphiphilic molecules. From Figure 1 it is seen that amphiphilic molecules or amphiphiles have distinct moieties of hydrophobic (water-repelling) and hydrophilic (water-attracting) character.

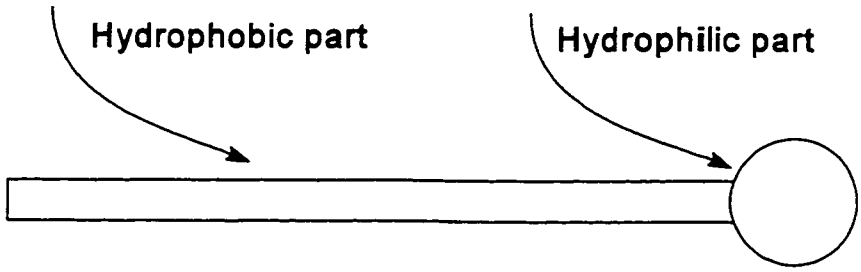

Figure 1. Schematic Representation of a Surfactant Molecule.

Generally, a hydrophobic domain is composed from long hydrocarbon chains (less often halogenated or oxygenated analogues), both straight and branched, or aromatics. Due to the nature of polar head group, four main types of surfactants are distinguished: neutral, anionic, cationic, and zwitterionic. Both hydrophobic and hydrophilic domains govern the different properties of surfactants: solubility, surface

activity, degree of packing of molecules at the interface, and stability. Among all properties surfactants possess one is of interest for the purposes of this work, and that is their ability to form molecular aggregates called micelles.

Micelles.

Structure and Physical Properties.

Self-association of the hydrophobic chains of monomeric surfactants in polar media, followed by desolvation, leads to a decrease in the free energy of the system, which is considered to be the main driving force for micelle formation[10, 11,12]. Such formation is a cooperative process that involves a large number of surfactant molecules[11] in order to achieve an effective elimination of the surfactant-polar solvent interface, and which establishes some lower limit to micellar size. On the other hand micelles cannot be infinitely large because of electrostatic repulsion between head groups of the same charge. In the case of neutral surfactants the preference for hydration of a head group opposes to the self-association. The average number of surfactant molecule forming a micelle usually lays between 50 and 100 and it depends on the nature of surfactant, temperature, and electrolyte concentration.

A large number of structural models of micelles have been proposed over last several decades, but some features are common to all of them. Figure 2 gives an idea about general structure of micellar aggregate.

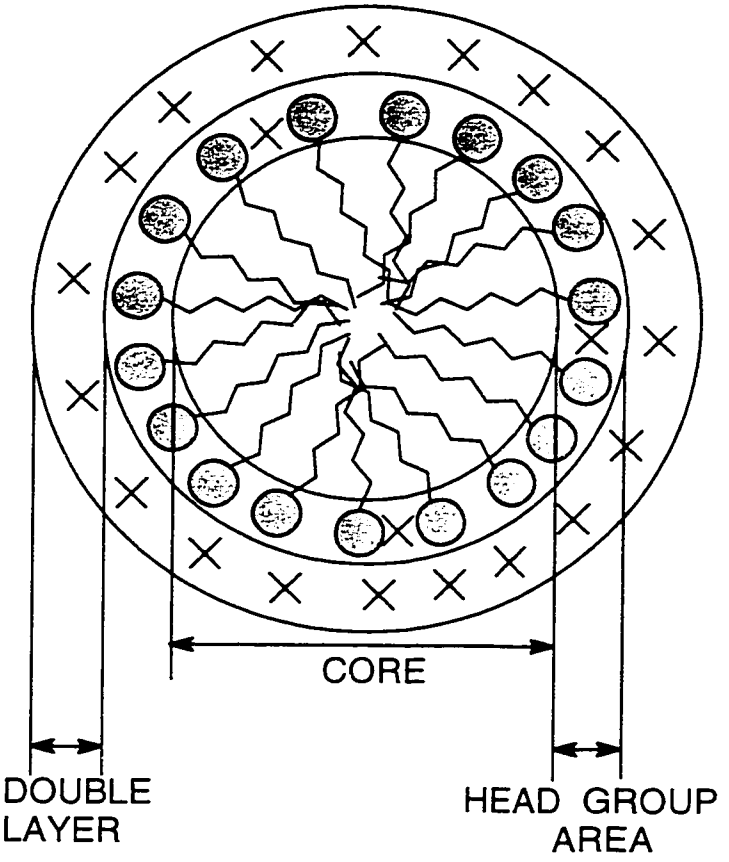

Figure 2. A Two-dimensional View of a Spherical Micelle.

Though the scheme above does not reflect exact relative location and configuration of micelle elements, three main regions can be seen: core, head group area, and electrical double layer. A micellar core is composed from hydrophobic tails of surfactant molecules, and is of 10-30Å in size. It is surrounded with head group area, called Stern layer, which is normally up to a few Å in thickness. Besides the polar head group, a little amount of counterions can be

found in the Stern layer. Both the core and the Stern Layer are sitting inside an electrical double layer, composed of counterions for the head groups. This part of micelle may reach up to 200Å in size.

As for the configuration adopted by surfactant units and their arrangement, several models have been proposed. The earliest one, known as the Hartley model[13], is characterized by a radial arrangement of hydrophobic chains, smooth micelle surface, little water penetration into the hydrophobic core, and minimal hydrocarbon-water contact at a micelle surface. This point of view was widely accepted for several decades. However, in the late 70's Menger showed[14] that a spherical micelle formed by straight chains of surfactant would have huge cavities. That gave rise to a Menger micelle, which presents following features[13]: a) a disorganized collection of surfactant molecules, and many of them are bent; b) a rough micelle surface with small water-filled pockets; c) the presence of hydrocarbon chains at the surface in direct contact with water. The net result is that the Menger micelle is much less organized than Hartley micelle. Many non-spherical models had been also proposed, and most common of them are cylindrical, rod-like (by Debye), lamellar (by McBain), and hexagonal[8] (Figure 3). Presently, due to development of NMR, ESR, etc., it is known, that with an increase in concentration of ionic surfactant, the micelle shape changes from spherical to lamellar, while passing through cylindrical and hexagonal. In the case of nonionic surfactants the shape of micelles changes directly from spherical to lamellar.

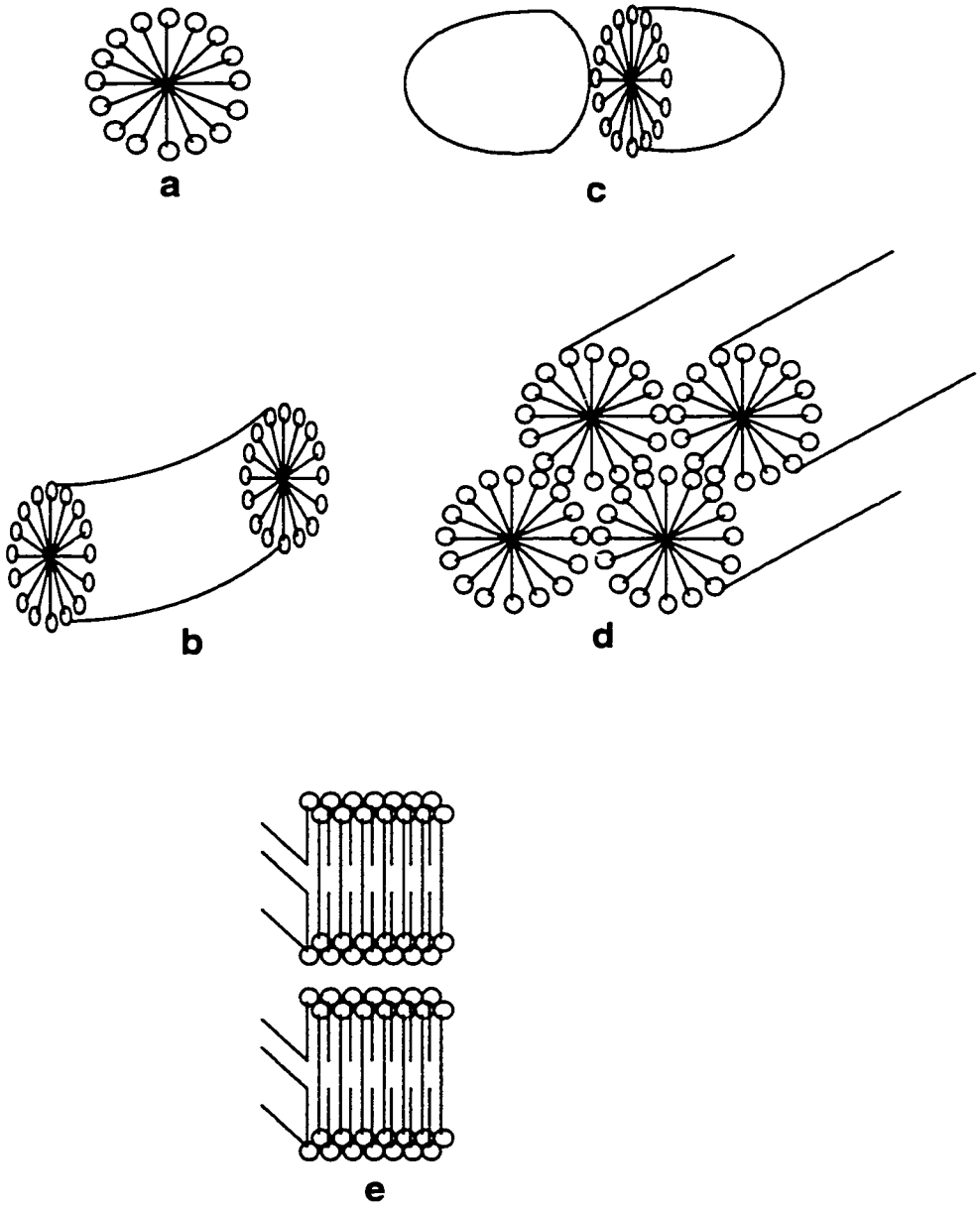

Figure 3. Possible shapes of micelles[12]: a) spherical (Hartley); b) cylindrical; c) rod-like (Debye); d) hexagonal; e) lamellar (McBain).

Critical Micelle Concentration.

As mentioned before, micelle formation involves a fairly specific number of surfactant molecules. This means that there exists a certain concentration, more precisely a narrow range of concentration, of surfactant at which micelles become detectable. Such a concentration is called *critical micelle concentration*, or CMC[10-12]. Micelle formation leads to abrupt changes in many properties of solution: conductivity, viscosity, pH, density, etc., and so in a plot of given property against surfactant concentration a change in the slope is generally observed (figure 4). The point of slope change on the plot corresponds to CMC.

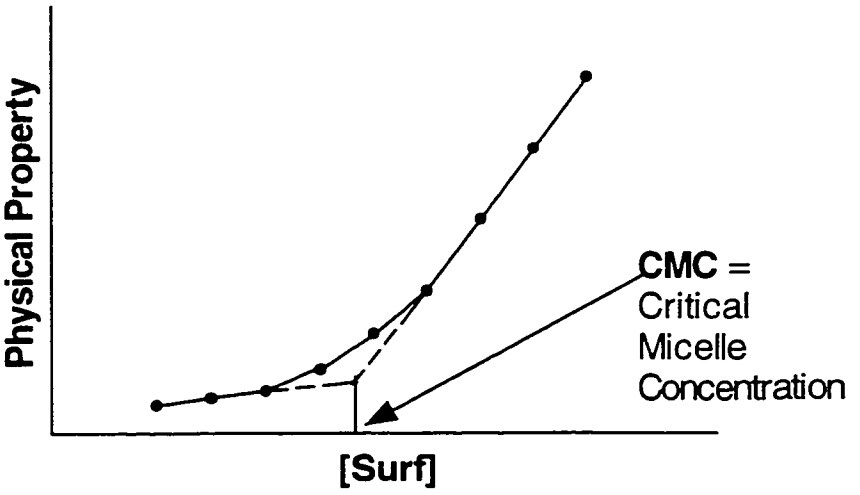

Figure 4. Graphical definition of critical micelle concentration.

CMC values depend on a number of different factors, such as nature of both hydrophobic and hydrophilic parts of surfactant molecules, type of environment (solvent and counterions), temperature, etc. For any homologous series of

surfactants, the dependence of CMC on the number of carbons in the hydrophobic chain is observed[9]. The equation can be written to describe this dependence:

$$\log(CMC) = A - BN \qquad (1),$$

where N is number of carbons in the surfactant chain, and coefficients A and B reflect the change in the free energy when transferring a molecule from aqueous environment to the micellar phase. The experimental value of CMC may depend somewhat on the measurement method, however, determining CMC with a high degree of accuracy is possible. For the majority of surfactants CMC values fall into the range 10^{-4} - 10^{-2} M[9,10].

Chemical Properties.

Micellar Effects on Chemical Reactions.

Above their CMC, in other words, after micelles being formed, solutions of surfactants may affect the rate of various chemical reactions. Within the last 30 years extensive data have been collected on micellar effect on chemical reactions[10,15]. Many processes, like ester cleavage[16-21], alkene bromination[22], acid-base equilibria[23], etc. were found to be subject to micellar influence. It was observed that micelles can either catalyse or inhibit reactions, with effect depending on the nature of the substrate, the reaction, and the micelle. Typical situations are

presented on Figure 5.

Because of easy spectroscopic detection of products, basic cleavage of *p*-nitrophenyl esters and acidic hydrolysis of acetals became invaluable tools in micelle research. Many properties of micelles were established using these and similar processes, so the following discussion deals mainly with such types of reactions.

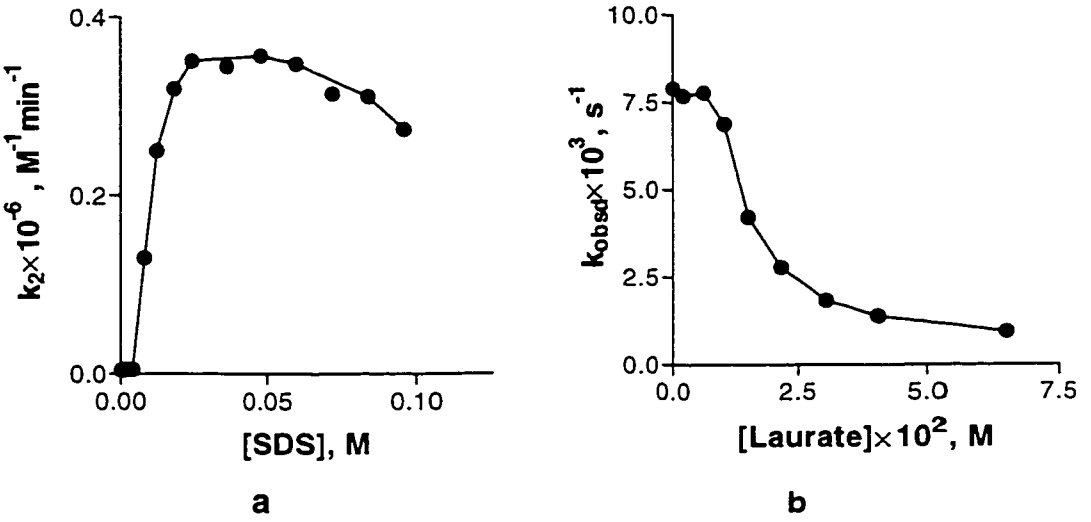

Figure 5. Examples of micellar effect on chemical reaction: a) hydrolysis of methylorthobenzoate in acidic aqueous solution in presence of sodium dodecyl sulfate (SDS)[16]; b) hydrolysis of mono-*p*-nitrophenyl dodecanedioate in basic solution in presence of laurate[17].

Sources of Rate Changes in Micellar Systems.

There are several reviews and surveys that cover reactive properties of micelles[10,15,24,25]. Two main features were established immediately: a) cationic micelles catalyse reactions where anionic nucleophiles involved (eg. basic cleavage

of esters) and inhibit reactions involving positive species (eg. acetal cleavage), while behaviour of anionic micelles is exactly opposite; b) the effect that micelles bring about is a function of the hydrophobicity of both the surfactant and the substrate. Thus, Menger and Portnoy found[17] that cleavage of *p*-nitrophenyl alkanoates by hydroxide ion is catalysed by micelles of cetyltrimethylammonium bromide (CTAB), and is inhibited in the presence of sodium dodecyl sulfate (SDS). Moreover, they established that the degree of catalysis was a function of acyl chain length in the ester, with longer esters being affected to the greater extent. Later, Quina and co-workers established[26] the same pattern for inhibition of hydrolysis of a series of *p*-nitrophenyl alkanoates in presence of SDS.

All these observations suggest that electrostatic and hydrophobic interactions govern the kinetics of organic reactions in micellar solution. It was suggested[24] that electrostatic forces were responsible for stabilization of transition state forming in the course of the reaction and for concentration of the attacking species. Obviously, both factors work in the same direction. For example, positive charge on the surface of cationic micelles that catalyse the basic cleavage of carboxylic esters, stabilizes negatively charged tetrahedral intermediate, and, at the same time, attracts hydroxide anions increasing their concentration in the vicinity of the reaction centre. Inhibition of the same reaction by anionic micelles can be understood in similar terms.

Hydrophobic interactions serve as binding forces between the micellar phase and reactants, transition states and products. Experimental data exist exhibiting the importance of hydrophobic interactions. For example, for hydrolysis of methyl

orthobenzoate it was found[25] that association of 50% of substrate within micellar phase corresponds approximately to 50% of a total rate increase. Another example is that the increase in catalytic efficiency of sodium alkyl sulphates in the order hexadecyl > tetradecyl > dodecyl > decyl > octyl[10,24].

Reaction Site Location.

Debates over the location of the reaction site in relation to micellar structure have lasted for years. It is now agreed, however, that most reactions occur in the Stern layer (figure 2) of the micelle. Many experimental data support this hypothesis. Among the most important ones is the observation that micelles do not affect the rate of chemical reaction if one of the reactants is drawn inside micellar phase and another stays in aqueous media[27]. Another fact is that inclusion of ions from a bulk phase to micellar interior have not been found. For the hydrolysis of a series of phenyl laurates it was found that the sensitivity of the reaction to the phenoxide leaving group is very similar in purely aqueous solution ($\beta = -0.56 \pm 0.05$) and in presence of a micellar catalyst ($\beta = -0.51 \pm 0.06$)[28]. That, of course, leads to a conclusion that reaction centre is outside of hydrophobic interior of a micelle. It should be noted here that there is not precise borderline between the micellar core and the Stern layer, and when referring to the location of a reaction site one speaks about predominant polar or non-polar environments.

Quantitative Treatment of Micellar Kinetics.

Kinetics in micellar solution exhibit saturation behaviour, i.e., the rate of a reaction changes with an increase in surfactant concentration, and then levels off. The pseudophase model, and its further development, the pseudophase ion-exchange (PIE) model, have been the main models employed to treat kinetic data in the presence of micelles.

The pseudophase model[17] was based on the assumptions that substrate is distributed between micellar pseudophase and aqueous solution, and that reaction of free and bound substrate occur independently with their own rate constants. Figure 6 gives the general scheme for such a process.

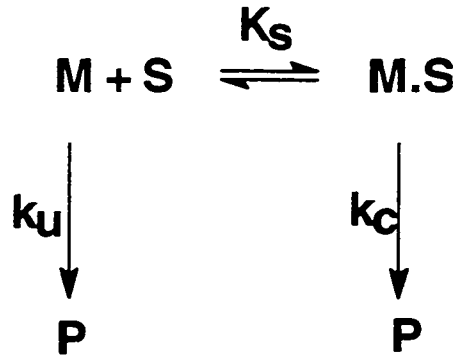

Figure 6. Kinetic Scheme for Micelle Catalysed Reaction.

In figure 6, K_S is a dissociation constant for the substrate-micelle complex, k_u is the rate constant for reaction in aqueous medium, and k_c is the rate constant of conversion of the substrate-micelle complex into the product. Combination of

kinetic equations corresponding to both processes gives the possibility to estimate an overall observed rate constant as a function of surfactant concentration, as shown in equation 2:

$$k_{obsd}=\frac{k_u K_S+k_c[Surf]}{K_S+[Surf]} \qquad (2)$$

In this equation [Surf] = $[Surf]_0$ - CMC, where $[Surf]_0$ is stoichiometric amount of surfactant. The number of data has been successfully treated using pseudophase model. In the monograph by Fendler and Fendler[10] a lot of examples were inspected.

It was found, however, that in many cases the maximum is observed on plots of $k_{obsd.}$ vs. surfactant concentration (see, for example, figure 5a), and equation 2 fails to describe experimental data. This is particularly true in case of micelle-assisted bimolecular reactions. Two reasons are responsible for such behaviour. The first one is the fact that in case of bimolecular reactions the binding of both reactants to a micelle must be taken into account, but this gives rise to a problem of defining concentration of reactants bound to micelle. At best, one ends up with determining of a mole ratio of one of the reactants between solvent and micellar phases[29]. Sometimes, by keeping concentration of one reactant in large excess

over another, it is possible to establish pseudo first order conditions and avoid this problem.

The second reason is competitive binding of an inactive counterion to the micelle. Beside the observed maximum in the rate constant-surfactant concentration profile, it was also found that addition of a salt suppresses catalysis by micelles[10,12,15,22]. Another observation was that different types of an active ion can displace each other from a micelle. Attempts to give the quantitive consideration to this problem gave rise to a pseudophase ion-exchange model. The cornerstone of this model is the assumption that a micelle surface is saturated by counterions and, therefore, the charge of a micelle per head group is a constant[29,30]. Thus, equilibrium constant for ion-exchange process can be defined:

$$K_{XY}=\frac{[Y^-]_W[X^-]_M}{[Y^-]_M[X^-]_W} \qquad (3)$$

It is not difficult now to find the concentration of a given reactive ion in the micelle using the parameter K_{XY} and assumed constancy of fractional micelle charge[29,30,31]. However, it is possible to conduct an experiment at a fixed ionic strength of solution, and to carry out fitting with the standard pseudophase model.

Dendrimers.

Structure and Physical Properties.

Dendrimers are branched-chain, three-dimensional macromolecules. This name came from similarity between such molecules and trees (*dendron* is a Greek word for tree). They also called cascade molecules. Around half a century ago, Flory[32,33] established theoretical background for the existence of such macromolecules, but only some forty years later developments in the synthetic technique allowed the creation of the first molecules of this type. Since then a large number of different dendrimers have been synthesized[34-37].

Despite their differences, all dendrimers have same structural features: a central core (or reference point), repeating units, and terminal (functional) groups (figure 7).

The core is a molecule possessing N_C reactive sites, where N_C is called the core multiplicity. Virtually any organic and inorganic molecule can be chosen as a core. As an examples NH_3 (N_C=3), ethylenediamine $H_2NCH_2CH_2NH_2$ (N_C=4), SiH_4 (N_C=4), and benzene C_6H_6 (N_C=3) could be mentioned. A repeating unit is a fragment of a molecule with N_R reactive sites, with the absolute requirement that N_R >1 to introduce multiplicity. As examples fragments like 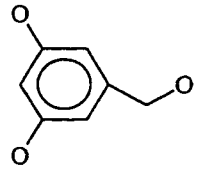 with N_R=2,

-$CH_2CH_2CONHCH_2CH_2N<$ with $N_R=2$, or -$C(CH_2OH)_4$ with $N_R=3$ could be chosen. The terminal group is simply any atom or molecule attached to the last repeating unit.

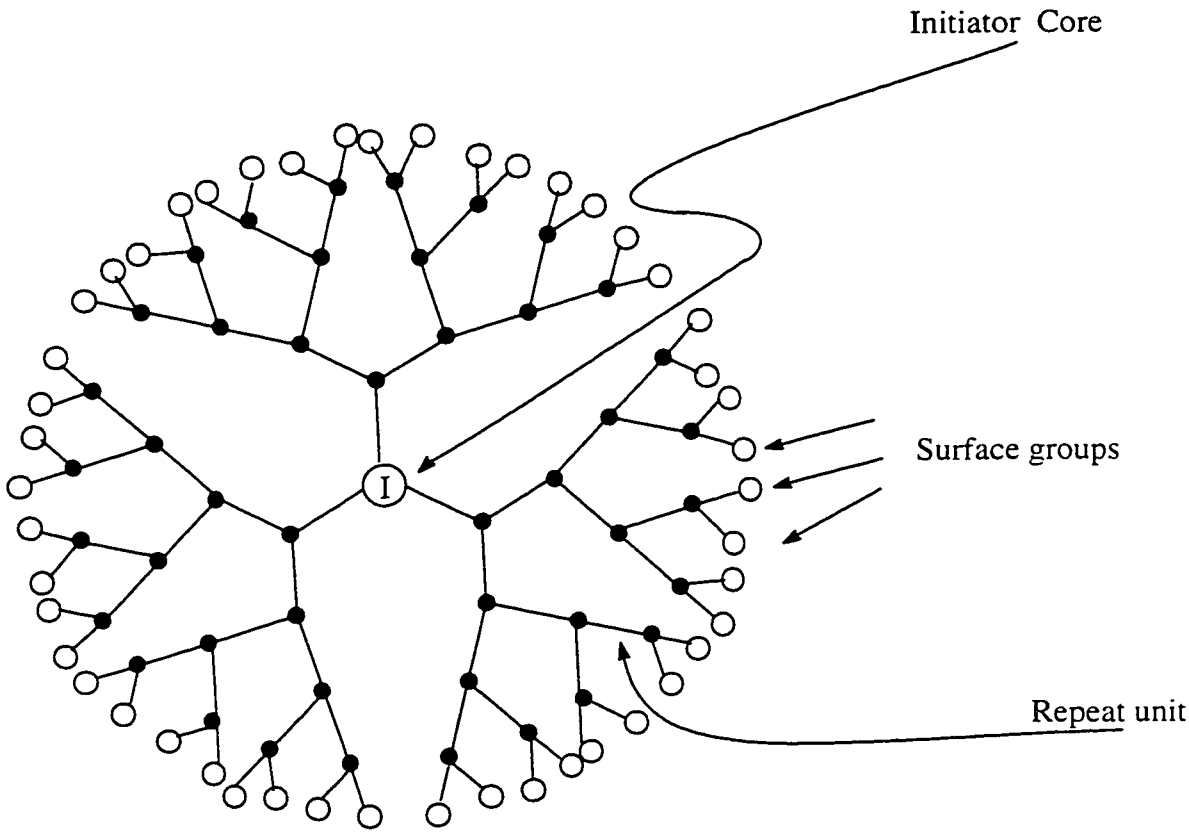

Figure 7. Schematic Representation of a Dendrimer Molecule.

The synthesis of a dendrimer is a mathematically precise procedure. Indeed, the number of terminal groups, repeating units (which is an equivalent to the degree of polymerisation), and molecular weight, all are direct functions of the initiator core multiplicity N_C and the branch-juncture multiplicity N_R (equations 4-6)[37]:

$$z=N_C N_R^G \tag{4}$$

$$N_{RU}=N_C\frac{N_R^{G+1}-1}{N_R-1} \tag{5}$$

$$M=M_C+N_C[M_{RU}\frac{N_R^{G+1}-1}{N_R-1}+M_T N_B^{G+1}] \tag{6}.$$

In these equations z is the number of terminal groups, N_{RU} is the number of repeating units, M, M_C, M_{RU}, and M_T are molecular masses of dendrimer, core, repeating unit, and terminal unit respectively, and G is the generation number (figure 8).

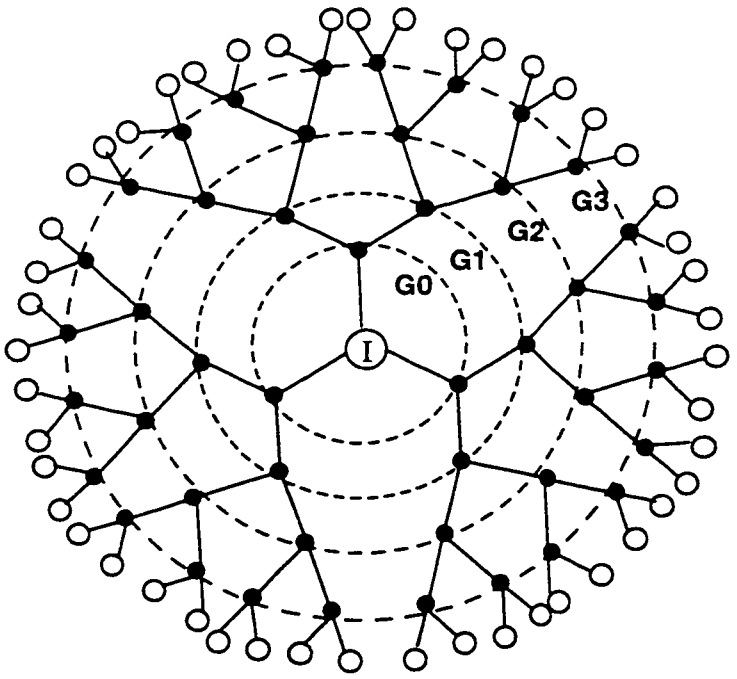

Figure 8. Definition of Generation for Dendrimers (G=Generation).

So the nature of the core and the repeating unit controls completely the final size, shape, and flexibility of a resulting dendrimer, properties known as critical molecular design parameters (CMDPs)[37]. Chemical properties, on the other hand, are controlled largely by the nature of the terminal groups.

It was suggested, and lately shown using computer simulation, that dendrimers of early generations possess open, starfish-shaped structure, but when growing to higher levels they become more rigid and close ball-shaped molecules[37]. Later still this was confirmed experimentally, using fluorescence probe and EPR techniques[38-40].

Chemical Properties and Possible Applications.

From the very beginning structural similarities between dendrimers and micelles were noted[37,38]. For example, both micelles and dendrimers have a very similar size - 10 - 300 Å. Both of them have a near spherical shape (except for the earliest dendrimer generations). Besides, the dependence of the terminal groups on generation number for dendrimers can be related to aggregation number of micelles. However, one important difference must be stressed: micelles are dynamic molecular aggregates, whereas dendrimers are discrete molecules (that is why they called sometimes "unimolecular micelles").

Given the existing similarities between micelles and dendrimers, it was natural to expect similar properties, at least partially. One of the fundamental properties of micelles is binding of different molecules, and recently the binding of

several guests to amino-acid functionalised dendrimers have been reported[41]. Tomalia *et al.* compared properties of anionic micelles and their unimolecular "analogues" - starburst PAMAM (see later) dendrimers[39]. Many similarities in behaviour were found, such as in the plots of intramicellar and intradendrimer quenching constants of a $Ru(phen)_3^{2+}$ probe as a function of alkyl chain length for micelles or generation number for dendrimers (figure 9).

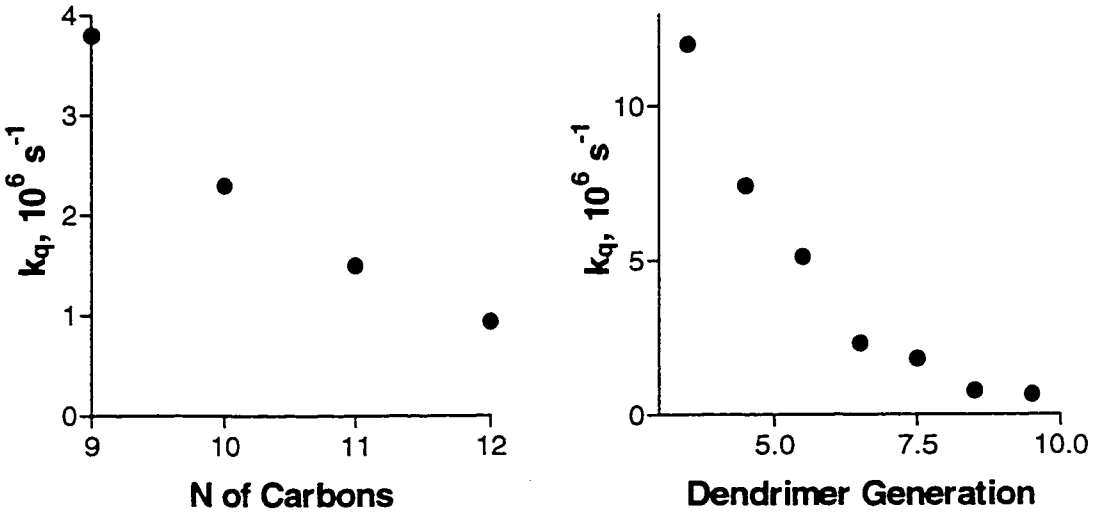

Figure 9. Plots of intramicellar and intradendrimer quenching constants of a $Ru(phen)_3^{2+}$ probe as a function of alkyl chain length for micelles or generation number for dendrimers.

Catalysis is not the only area of dendrimer application. Although dendrimer properties have been studied only for a relatively small period of time, it has been proposed that dendrimers can be used as size standards in size-exclusion chromatography, carriers in electrokinetic chromatography, solubilizing agents, drug carriers, and antibody conjugates in biology and biochemistry, and to have

applications in many other fields of scientific and industrial activity[34,42]. Each application depends, of course, on the origin and nature of a particular dendrimer.

Cyclodextrins.

Structure and Physical Properties.

Discovered in 1891 by Villiers[43,44], cyclodextrins have attracted the attention of scientists for more than century, with many groups actively investigating their chemistry within the last few decades. This level of interest can be easily understood if we consider present and potential applications of cyclodextrins in science and industry[44,45].

The family of cyclodextrins consists of 6 or more D-glucose[44,45,46] units, linked α-(1,4), as in amylose. The three most major forms are those with 6, 7 and 8 glucose units, which are referred to as α-, β-, and γ-cyclodextrin, respectively. The schematic formula of cyclodextrin is shown on figure 10.

As can be seen from figure 10, cyclodextrins (CDs) are toroidally shaped molecules, having the form of a bottomless "nanobucket". This shape is due to the α-1,4-linkage between glucose units, which are roughly in the relatively undistorted C1 chair conformation (figure 11). The linkage between glucose units has special implications on the arrangement of functional groups in cyclodextrin, and it is this particular arrangement that leads to a wide range of interesting properties of cyclodextrins. The cyclodextrin cavity has "V"- shape where the secondary hydroxy

groups are on the wider opening of the cavity and the primary hydroxy groups are on the narrow side (figure 10). It should also be noted that the primary hydroxy groups and attached methylenes can rotate, while the secondary ones are relatively fixed.

The structural features of cyclodextrins are supported by X-ray crystallography[47] and by indirect chemical evidence: a) molecular weights are integral multiples of the value for a glucose residue (M.W.=162.1);[48] b) the only product of acid hydrolysis of cyclodextrins is glucose;[44,48] c) permethylation of the cyclodextrin followed by hydrolysis yields only 2,3,6-trimethyl glucose[44,48].

Both primary and secondary hydroxy groups are completely outside of cyclodextrin molecule. The interior of the CD cavity is lined with C-H groups and glycosidic oxygens, which make the cavity of cyclodextrin bucket relatively apolar, which in turn leads to most of the important properties of CDs.

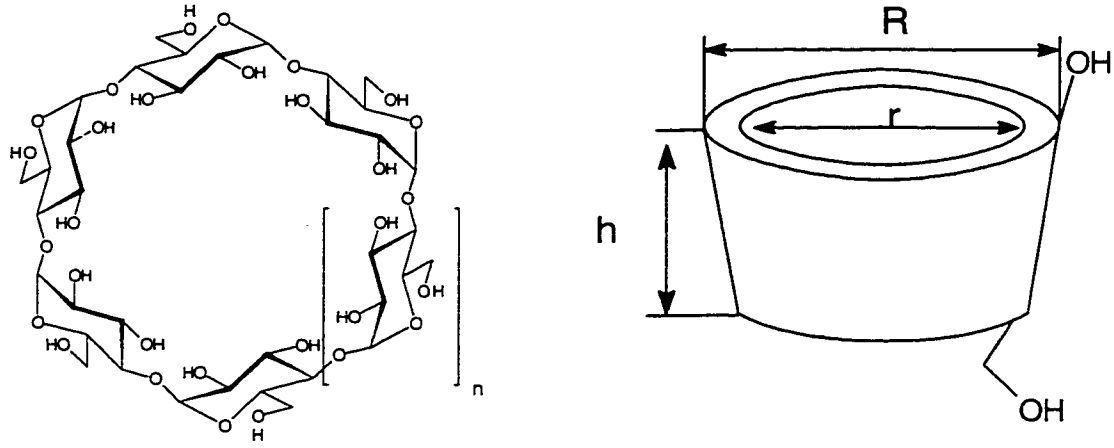

CD	n	R,Å	r,Å	h,Å
α	1	13.7	5.7	7.8
β	2	15.3	7.8	7.8
γ	3	16.9	9.5	7.8

Figure 10. General structure, shape and size of α-, β-, and γ-cyclodextrin

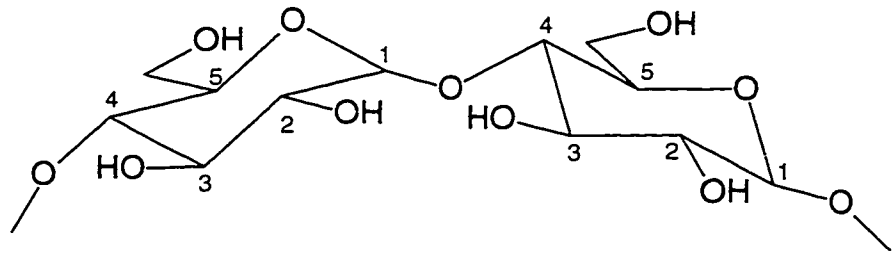

Figure 11. Structure of 2 glucose units in a cyclodextrin molecule.

Chemical Properties of Cyclodextrins

The most valuable properties of CDs are those due to their ability to form inclusion complexes. In such complexes CDs serve as the host and can include into their cavities a variety of different guests. The different sizes of α, β and γ-CD mean that the cyclodextrins are capable of binding a wide variety of compounds, ranging in size from small inorganic ions up to vitamin A derivatives[43-45,49,50]. As an approximate rule, the cavity of α-CD is of appropriate size to include benzene derivatives, while β-CD and γ-CD are more suited for naphthyl and anthracenyl derivatives, respectively.

The main binding forces of host-guest complexes of cyclodextrins are in general the same as for other inclusion complexes[2,3], however, there are other factors which must be taken into account. It has been shown that release of "high energy" water molecules plays a very significant role in formation of complexes in aqueous solution[44,51]. When a guest binds in the CD cavity, these energy water molecules are returned to bulk solvent, thus lowering the overall energy of the system. Another important consideration is release of strain energy in the macromolecular ring of the CD[52]. The conformation of the CD-ring in aqueous solution before complex formation is less symmetrical and, thus, of higher energy than one after complexation. Evidence supporting the formation of inclusion complexes was obtained by many methods,[43-45,48] including proton nuclear magnetic resonance spectroscopy[51] and fluorescence measurements[53].

The primary role of hydrophobic effect in CD complexes formation was

established by studying correlations between strength of binding of different aliphatic compounds and alkyl chain length[5,54-56]. Such a correlation can be considered as a linear free energy relationship (LFER)[5]. Studies of alcohols, ketones, aliphatic amines, alkanoate and alkanesulphonate ions showed that strength of binding increases with increase in number of carbons in alkyl chain up to C_8. Moreover, all these correlations in the form of a plot of pK_S vs. N (where K_S is dissociation constant of CD complex, and N number of carbons in alkyl chain) are straight lines, with slopes between 0.3 and 0.5. The Gibbs energy, corresponding to these slopes, is 2-3 kJ/mol for transfer of one methylene group from aqueous solution to the CD cavity, which is very close to the value of free energy of transfer of a methylene group from polar to various non-polar organic media[11].

Cyclodextrins have been shown to affect the rates of a great number of chemical reactions[43-46]. This effect is intimately linked with the ability to form inclusion complexes with the substrates, which was evidenced by the following general observations[44]: a) the rate of a reaction approach a maximum with increasing [CD], indicating saturation-type kinetics; b) the effect of the CD on the reaction is inhibited by the compounds which bind to the CD (but do not react with the substrate); c) α-methyl glucoside has no effect on reactions that are catalyzed by cyclodextrins (or it exhibits a very small effect).

Cyclodextrins can accelerate reactions by either covalent or non-covalent catalysis. Table 1[43,44] gives an overview of some cyclodextrin catalysed reactions.

Table 1. The Overview of Cyclodextrin Catalysed Reactions.

Reaction	Substrate	Acceleration	Type of catalysis[a]
Hydrolysis	Phenyl esters	300	C
	Penicillin	89	C
	N-acylimidazole	50	C
	Aryl carbonates	19	N
Decarboxylation	Cyanoacetate ion	44	N
Oxidation	Hydroxyketones	3	N

a) C covalent catalysis; N non-covalent catalysis

Covalent catalysis occurs when there is a distinct covalent intermediate formed between the cyclodextrin and the substrate. This usually involves the nucleophilic attack of one of the CD hydroxy groups on the substrate. One of the most studied examples of covalent catalysis of this type is the cleavage of phenyl esters[5,43-45].

Non-covalent catalysis can be attributed to either "microsolvent effects", due to the nature of CD cavity, or to conformational effects, due to geometric requirements of inclusion. An example of the "microsolvent effect" is the catalysis afforded to the decarboxylation of cyanoacetic acids[57,58], while conformational catalysis is observed in a CD - catalysed intramolecular acyl transfer[43].

In either case, cyclodextrins bring a stabilization of transition state of a

catalysed reaction, relative to the initial state. Since catalyses by cyclodextrins is linked to their ability to form host-guest complexes, it would be safe to suggest that TS stabilization is also depends on the same property, at least partially. Studies of TS stabilization as a function of substrate structure using the Kurz approach (which will be discussed later) have proved it to be extremely a valuable tool in reaction mechanism determination. For example, using the correlation between alkyl chain length and TS binding, different geometries for transition state for reaction of cleavage of *p*-nitro and *m*-nitrophenyl alkanoates have been proposed[56].

Probe Reactions.

Two reactions have been chosen to probe properties of three macromolecules mentioned above, one to work under basic conditions, and the other for acidic ones.

In the former case, the reaction of cleavage of *p*-nitrophenyl alkanoates was employed (figure 12).

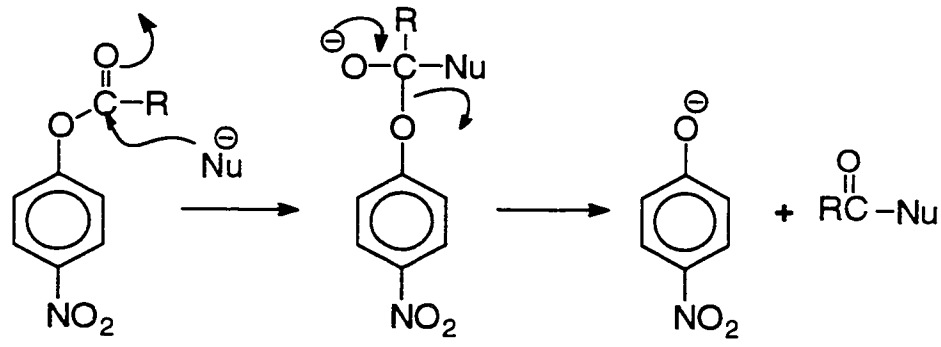

Figure 12. The cleavage of *a p*-nitrophenyl ester by a nucleophile.

This reaction belongs to the well studied class of carboxylic esters cleavage reactions. The initial attack of nucleophile (OH^- in the case of an aqueous solution of a base) leads to a formation of tetrahedral intermediate, which is further decomposes into products. In the case of *p*-nitrophenyl alkanoates, one of the products is the *p*-nitrophenoxide anion, which very easy to follow spectroscopically.

Another useful reaction is the acid catalyzed hydrolysis of acetals and orthoesters (figure 13).

In case of orthoester hydrolysis, the product is a carboxylic ester, if it is an acetal that is being cleaved the product is an aldehyde or a ketone. In either case, the reaction again can be easily monitored spectroscopically, when the substrates are aromatic.

The reaction of acetal (or orthoester) cleavage has been studied widely[59-64]. It is postulated that hydrolysis proceeds via carboxonium ion and hemiacetals as intermediates. The first step is acid catalyzed, but hemiacetal decomposition is catalyzed by both acids and bases.

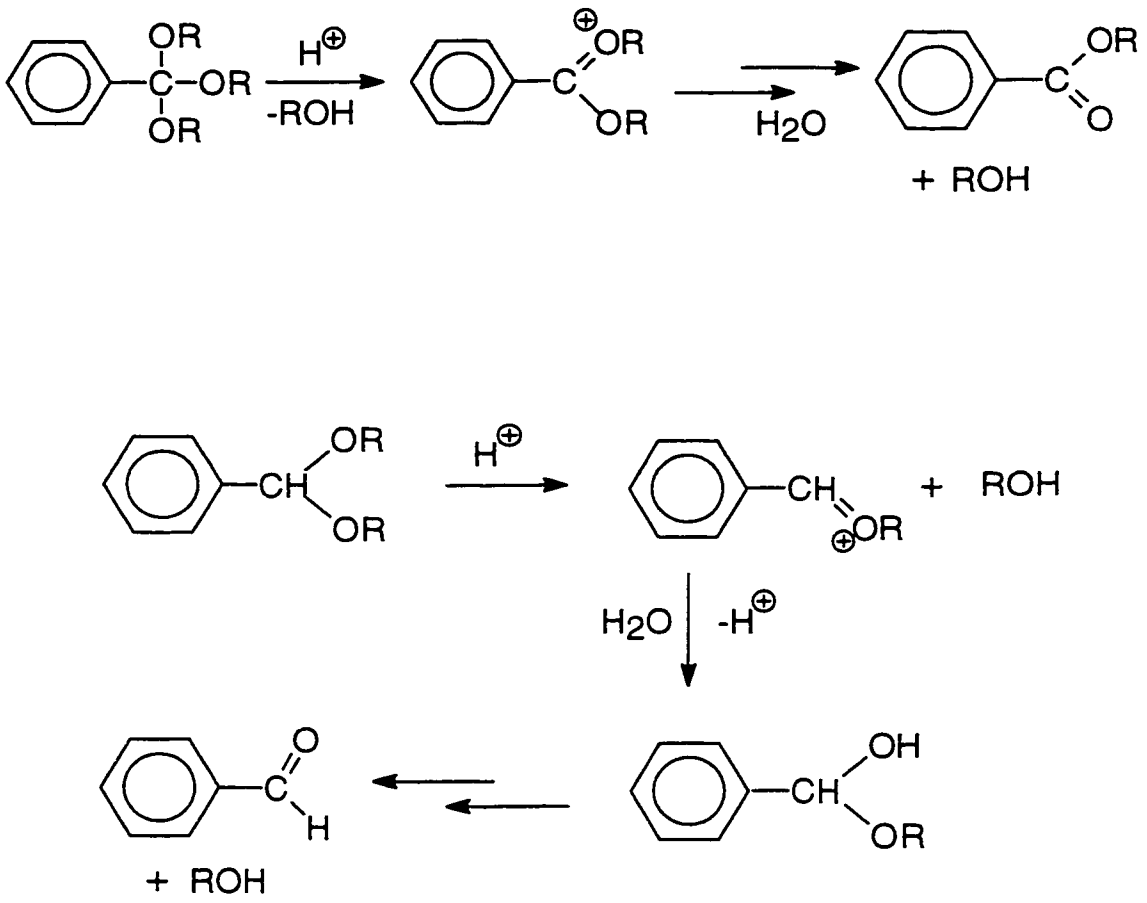

Figure 13. General Scheme for Acetal and Orthoester Hydrolysis.

Transition State Stabilization.

Catalysis of a reaction in general results from stabilization of the transition state of this reaction by a catalyst[5]. Any method that would help study of the transition state stabilization as a function of different reaction parameters gives a valuable tool to understand the process of catalysis itself. Such a method was found by Kurz[65].

The idea of this method is to consider catalysed and uncatalyzed processes (equations 7 and 8, respectively). Transition state theory[66] gives expressions for the rate constant for both processes, as in equations 9 and 10. Two assumptions are also made. First, the concept of transition state of reaction bound to a catalyst, TS.C is introduced. Also, the frequency of passage over the energy barrier, which is expressed as $v = k_b{}^*T/h$, is considered to be the same for both processes. Using these assumptions, equation 11 can be obtained dividing equation 9 by equation 10. In these equations, k_c is the rate constant for reaction of the complex S.C, and K_S is its dissociation constant. Consequently, $k_2 = k_c/K_S$ where appropriate.

$$S \xrightarrow{k_u} P \qquad 7$$

$$S + C \xrightarrow{k_2} P \qquad 8$$

$$k_u = v\frac{[TS]}{[S]} \qquad 9$$

$$k_2 = v\frac{[TS.C]}{[S][C]} \qquad 10$$

$$K_{TS} = \frac{[TS][C]}{[TS.C]} = \frac{k_u}{k_2} = \frac{k_u K_S}{k_c} \qquad 11$$

In equation 11 K_{TS} is the apparent dissociation constant defined by process

expressed by the hypothetical equilibrium in equation 12.

$$TS.C \rightleftharpoons TS + C \qquad 12$$

The greatest value of this method is that all the derivations were made without any assumptions regarding any mechanism. It should be noted, though, that K_{TS} is a quasi-constant. The formation and subsequently dissociation of complex like TS.C is very unlikely, but from the point of view of free energy, K_{TS} has a physical meaning: it is a stabilization of transition state that the catalyst brings to the reaction (figure 14).

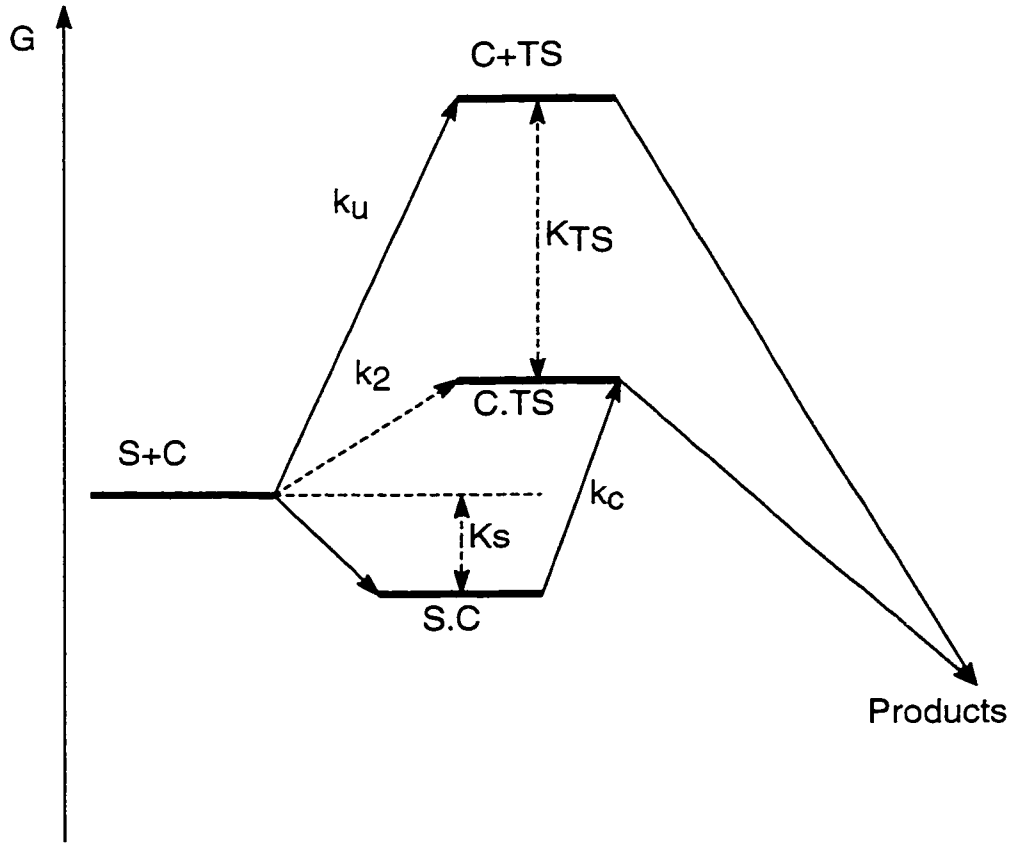

Figure 14. Gibbs Energy Diagram for Catalysed and Uncatalyzed Processes.

As it is seen from the diagram above, K_{TS} is directly related to a difference in free energies, given by:

$$\Delta G^{\circ}_{TS} = -RT\ln(K_{TS}) \qquad 13$$

Equation 11 can also be rewritten as follows:

$$\frac{k_c}{k_u} = \frac{K_S}{K_{TS}} \qquad 14,$$

from which it is seen now that the maximum acceleration for the reaction, k_c/k_u, depends on the relative binding strength of a substrate and a transition state to the catalyst. If transition state binds to the catalyst much stronger than substrate, than catalysis is expected to be large. If opposite is true, than inhibition is expected. Both types of situation are now well-known.

Results.

Reactions Mediated by Micelles.

Cleavage of *p*-Nitrophenyl Alkanoates.

Kinetic measurements of hydrolysis of a series of *p*-nitrophenyl alkanoates were carried out in phosphate buffer of pH=11.6 in presence of micelles of cetyltrimethylammonium bromide (CTAB). The raw data are collected in Appendix 1. Over the range of concentrations of CTAB the bromide concentration was kept at the constant value of 5 mM by addition of sodium bromide. The reaction was monitored by pseudo first-order release of *p*-nitrophenolate anion. Since $[Br^-]$ was constant, and the condition of $[ester]_0 << [surfactant]$ was applied, the reaction exhibited, as expected, saturation type of behaviour with respect to the CTAB concentration for all esters (figure 15). In order to facilitate the comparison, relative rate constants are plotted vs. [CTAB] in the figure.

The observed data were analysed by fitting the equation 2 to the data using non-linear least square analysis, and parameters K_S and k_c were estimated. Measured and calculated parameters are shown in table 2. Use of equation 2 is based on the simple pseudophase model. Experimental conditions (constant bromide anion concentration, large excess of surfactant over substrate) allow use of this model. Also, the correction $[CTAB] = ([CTAB]_o - cmc)$ was not made because the critical micelle concentration of CTAB is extremely small under the reaction conditions[9].

Table 2. Constants for the Cleavage of *p*-Nitrophenyl Alkanoates in Presence of CTAB Micelles[a].

Ester	k_U, s^{-1}	K_S, mM	k_C, s^{-1}
C_2	0.110	11.4±0.6	0.301±0.008
C_3	0.107	5.29±0.17	0.236±0.003
C_4	0.0693	1.96±0.10	0.161±0.002
C_5	0.0697	0.769±0.014	0.160±0.001
C_6	0.0649	0.257±0.013	0.160±0.001
C_7	0.0630	0.0819±0.0021	0.162±0.001
C_8	0.0591	0.0423±0.0031	0.147±0.002

a) in aqueous 0.2M phosphate buffer, pH=11.6, at 25 ± 0.1 °C. k_u values were obtained experimentally, K_S and k_c from fitting of equation 2 to observed data.

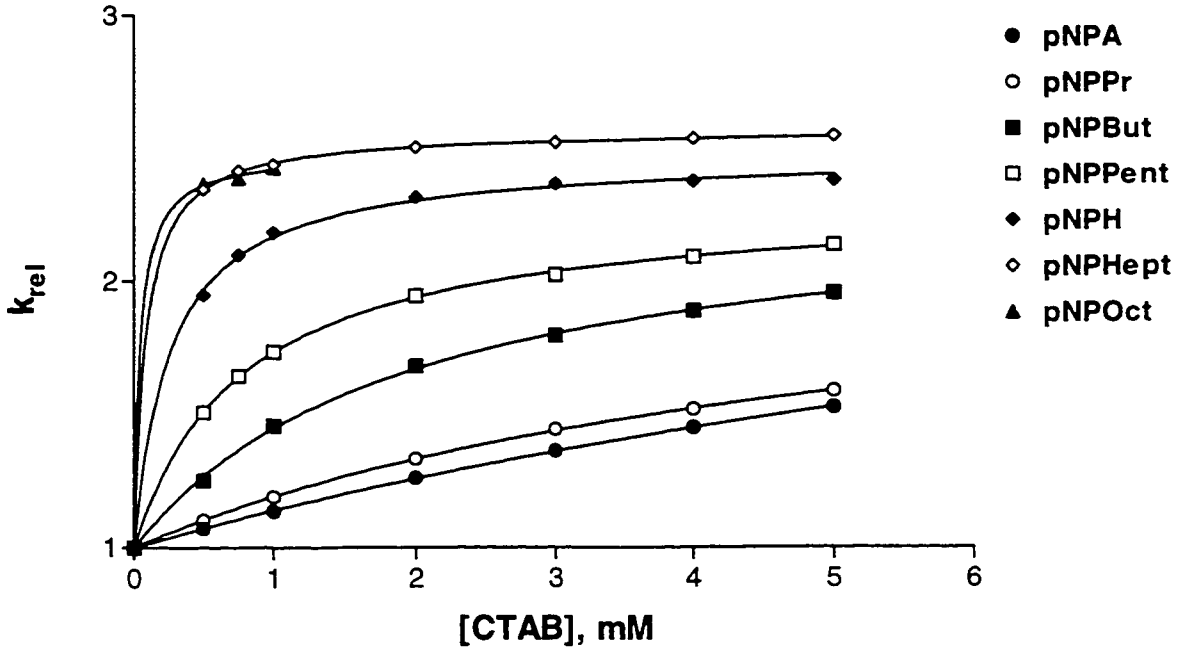

Figure 15. Dependence of Relative Rate Constant for Cleavage of *p*-Nitrophenyl Alkanoates on CTAB concentration.

The same type of measurements were performed with series of *p*-nitrophenyl alkanoates from acetate to hexanoate, but in the presence of anionic micelles of sodium dodecyl sulfate, SDS. Again, for all esters the saturation behaviour was observed (figure 16), but the reactions were inhibited by SDS. The corresponding K_S, k_c, and k_u parameters are collected in table 3. The raw data are collected in Appendix 1.

Since CMC value of SDS is not as small as for CTAB, it was necessary to use a corrected surfactant concentration, and for the fitting process the modified equation 2 was used:

$$k_{obsd} = \frac{k_u K_S + k_c([Surf] - CMC)}{K_S + ([Surf] - CMC)} \qquad 15$$

Table 3. Constants for the Cleavage of *p*-Nitrophenyl Alkanoates in Presence of SDS Micelles[a].

Ester	k_U, s^{-1}	K_S, mM	k_C, s^{-1}
C_2	0.104	19.8±3.1	$(1.76\pm0.10)\times10^{-3}$
C_3	0.0996	9.29±0.46	0[b]
C_4	0.0649	3.10±0.01	$(1.56\pm0.01)\times10^{-3}$
C_5	0.0653	1.24±0.01	$(3.90\pm0.12)\times10^{-4}$
C_6	0.0532	0.544±0.009	$(1.47\pm0.66)\times10^{-4}$

a) in aqueous 0.1M phosphate buffer, pH=11.6, at 25 ± 0.1 °C. k_u values were obtained experimentally, K_S and k_c from fitting of equation 15 to observed data. CMC was held as a constant at 1mM[9]; b) the actual value is $(-2.78\pm2.22)\times10^{-3}$.

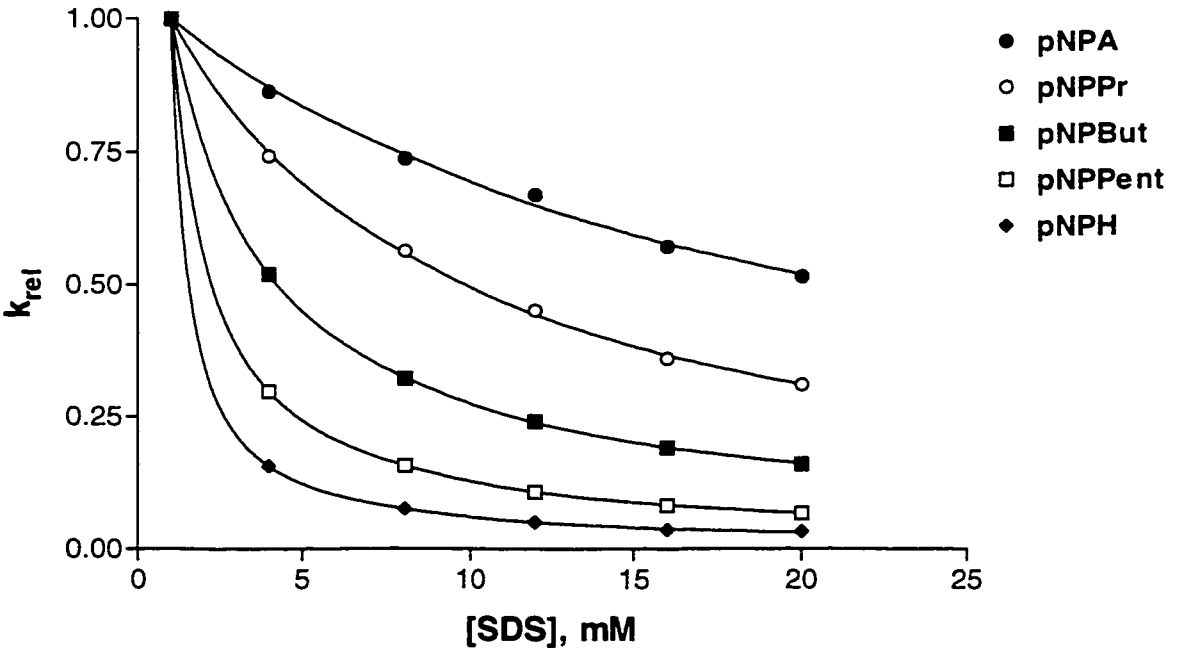

Figure 16. Dependence of Relative Rate Constant for Cleavage of *p*-Nitrophenyl Alkanoates on SDS concentration.

Discussion.

The reaction of cleavage of *p*-nitrophenyl alkanoates in presence of both cationic and anionic micelles is among the most studied[14,17,26]. Briefly, everything studied about these reaction can be summarized as follows:

a) Cationic micelles catalyse the cleavage of *p*-nitrophenyl alkanoates by hydroxide ion, whereas anionic micelles inhibit it;

b) The strength of binding of esters towards micelles is a function of acyl chain length, and increases as chain length becomes larger;

c) The magnitude of catalysis or inhibition is a function of acyl chain length as well. Both catalysis and inhibition are larger for esters with a larger acyl chain.

Unfortunately, all previous studies were performed on a limited basis, and the number of esters studied varied from one to maximum three. Also, to estimate the magnitude of catalysis the maximum *observed* catalysis was used in each particular case, since plots of observed rate constant vs. surfactant concentration usually have bell shapes, unless concentration of counterions was held at a constant value.

In this work, the systematic investigation of the reaction being discussed was performed. Since the large series of esters, from C_2 to C_8 (in case of SDS to C_6) was used, this allowed the influence of substrate structure on reaction parameters to be established much more precisely. Also, development of computer software allowed to estimate the parameter k_c, the maximum *theoretical* rate constant for the

system being studied, which in turn gives the possibility to calculate the ratio k_c/k_u, the maximum *theoretical* magnitude of catalysis ($k_c/k_u>0$) or inhibition ($k_c/k_u<0$).

As expected, it was found that CTAB micelles (cationic) catalyse the cleavage of p-nitrophenyl alkanoates, and SDS micelles (anionic) inhibit this reaction. From the data presented in tables 2 and 3, it is seen that the strength of binding of the esters to both CTAB and SDS increases as the acyl chain length grows. It was already noted, that in cases when hydrophobic effect plays primary role in process of binding, the plot of pKs vs. Acyl chain length is a straight line. Figure 17 represents such a plot for the binding of *p*-nitrophenyl alkanoates to CTAB and SDS micelles. The slopes of the lines in figure 17 are 0.421 ± 0.011 for CTAB and 0.400 ± 0.012 for SDS, which are very close and then suggest that in both cases very similar forces operate. These values are also similar to those obtained for other processes, where the hydrophobic effect is involved (see "Cyclodextrins" section in the introduction). The fact that the line for CTAB is slightly higher than one for SDS (and hence the binding of the same ester is stronger for CTAB than SDS) may be a reflection of different size of the surfactant hydrophobic chain: 16 carbons for CTAB and 12 for SDS.

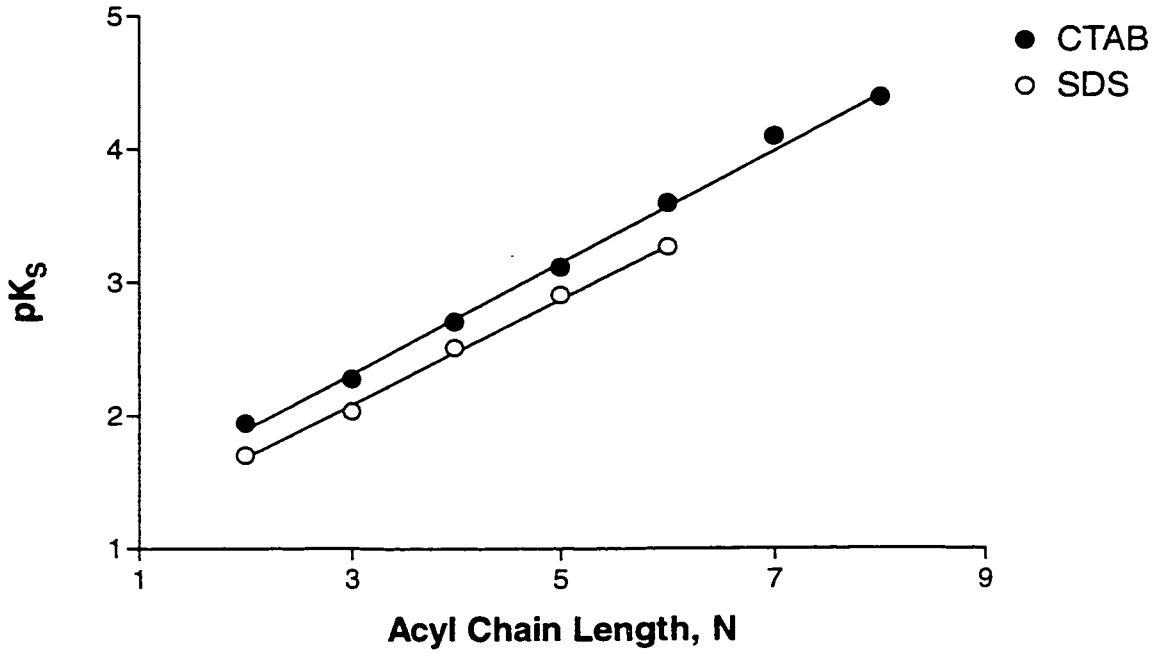

Figure 17. The Dependence of *p*-Nitrophenyl Alkanoates Binding Strength (pK_S) to CTAB and SDS on the Ester Acyl Chain Length.

Discussion of the chemistry of hydrolysis of the esters in the presence of micelles requires consideration of the parameters k_c/k_u, k_2, and pK_{TS}=-Log(K_{TS}), which are defined in equations 2 and 11, and illustrated in figure 14. For the cleavage of *p*-nitrophenyl alkanoates in presence of CTAB and SDS these parameters are collected in tables 4 and 5.

As has already been mentioned, previous studies showed that the magnitude of catalysis (or inhibition) was sensitive to the substrate's acyl chain length. However, with use of k_c/k_u as a probe of magnitude of reaction rate changes, different trends were established. For the CTAB mediated reaction the strength of catalysis k_c/k_u is fairly constant, being about 2.4 ± 0.3 for all seven esters (table 4). Moreover, there is no obvious dependence of this parameter on the ester structure. In fact, the plot of log(k_c/k_u) vs. acyl chain length is an almost horizontal line with a slope about 0 (figure 18). The same observations can be made in case of SDS mediated reactions. Although the rate is close to zero when [SDS] approaches infinity and thus it is impossible to derive K_{TS} and k_2 precisely, the estimation of k_c/k_u is still possible. Again, this parameter is independent on the substrate structure, and the plot of log(k_c/k_u) vs. N is an almost horizontal straight line with a slope about 0.

Table 4. Calculated Constants for the Cleavage of *p*-Nitrophenyl Alkanoates in Presence of CTAB Micelles[a].

Ester	k_C/k_U	k_2, $M^{-1}s^{-1}$	K_{TS}, mM
C_2	2.73	26.4	4.17
C_3	2.21	44.6	2.39
C_4	2.33	82.1	0.844
C_5	2.30	208	0.335
C_6	2.47	623	0.104
C_7	2.56	1980	0.0319
C_8	2.48	3480	0.0170

Table 5. Calculated Constants for the Cleavage of *p*-Nitrophenyl Alkanoates in Presence of SDS Micelles[a].

Ester	k_C/k_U
C_2	0.017
C_3	0
C_4	0.024
C_5	0.006
C_6	0.003

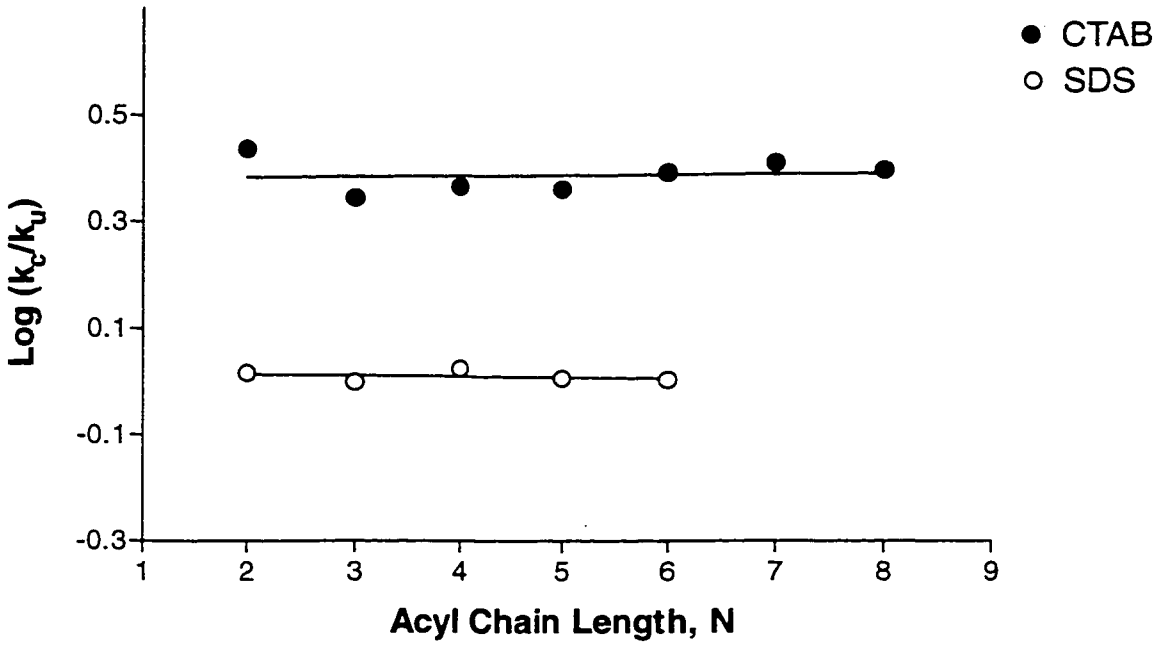

Figure 18. Plot of log(k_c/k_u) vs. Ester Acyl Chain Length for the Cleavage of *p*-Nitrophenyl Alkanoates in Presence of CTAB and SDS Micelles.

The explanation for this observation resides in the dependence of the transition state stabilization on acyl chain length. It is seen from table 4, that K_{TS} is sensitive to the number of carbons in acyl chain, and it decreases with the growth of this chain. The plot of pK_{TS} vs. N is straight line with a slope of 0.422 ± 0.016 (figure 19), which is the same as the slope of the dependence of pK_S vs. N. In fact, the correlation between pK_S and pK_{TS} is quite linear, with a slope of 1.00 ± 0.01(figure 20). Note that according to the equation 14, the similar sensitivity of both pK_S and pK_{TS} to structure predetermines the ratio k_c/k_u to be approximately constant.

From the other hand, the selectivity k_2 of CTAB for the different esters largely depends on the substrate binding, since $k_2 = k_u/K_S$, and k_u does not vary much. Consequently, k_2 increases from 26 M^{-1} s^{-1} for pNPA to 3480 M^{-1} s^{-1} for pNPOct, indicating that inclusion of the acyl chain of the esters enhance ester cleavage.

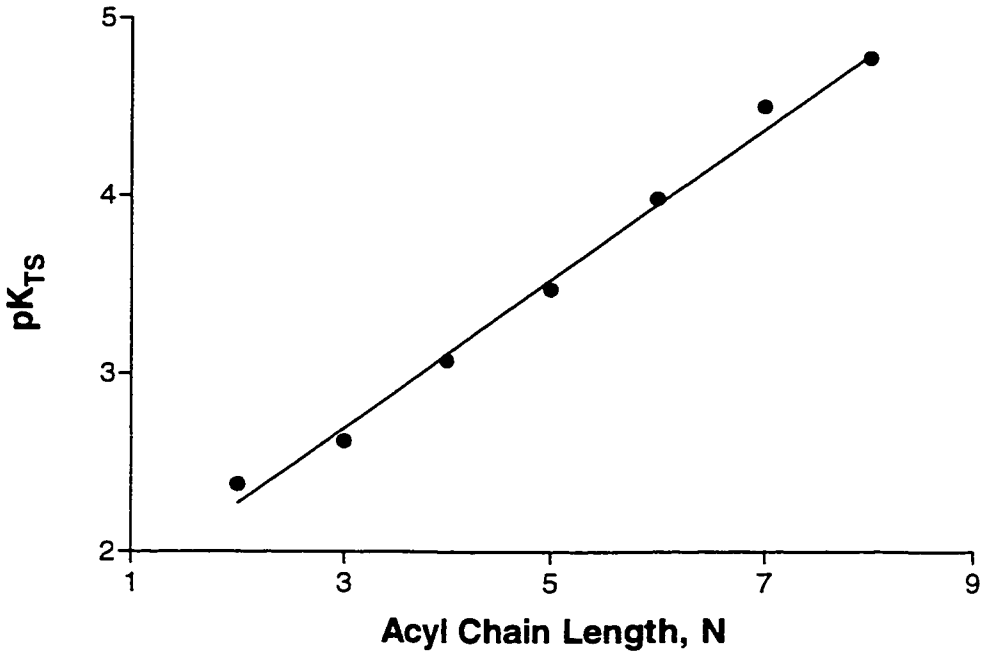

Figure 19. Acyl Chain Length Dependence of Transition State Stabilization (pK_{TS}) for the Cleavage of *p*-Nitrophenyl Alkanoates in Presence of CTAB Micelles.

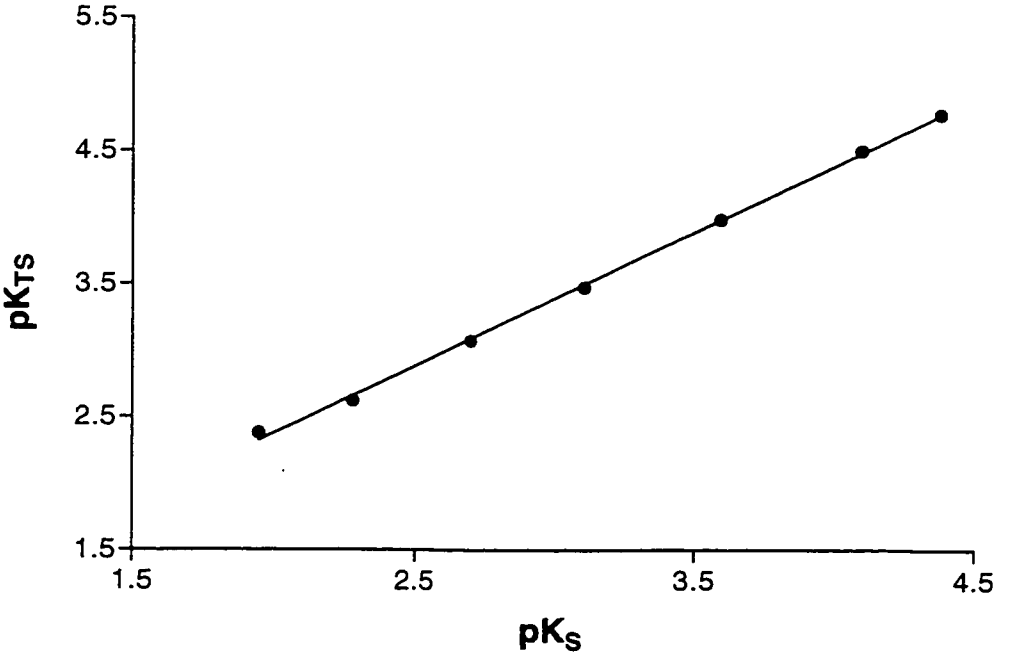

Figure 20. Correlation Between Substrate and Transition State Binding to CTAB for the Cleavage of *p*-Nitrophenyl Alkanoates.

Hydrolysis of Acetals and Orthoesters.

According to earlier studies, SDS micelles catalyse the acid-catalyzed hydrolysis of acetals and orthoesters. Although close consideration was given to this type of reaction previously, the analysis from the point of view of TS stabilization was not carried out before.

Two series of acetals were chosen for kinetic studies (figure 21).

Figure 21. General Structure of Acetals used for Studies.

In one series substituents directly attached to the carbonyl carbon, which is reaction centre, were varied (figure 21a). Substituents R=H, CH_3, and OCH_3 were used. In the case of OCH_3, the resulting compound is called an orthoester.

The second series of acetals was based on different substituents in the phenyl ring. As X substituent *p*-Cl, *m*-Cl, H, *p*-Bu, and *p*-OMe were chosen. The reaction was monitored by pseudo first-order appearance of resulting ketone or aldehyde in case of acetal, or benzoate ester in case of the orthoester. Raw data for these experiment are collected in Appendix 2. All traces of Absorbance vs. Time

showed initial induction period, which is a characteristic for two-step consecutive reactions[60] (figure 22). Early studies showed[64] that the second step, decomposition of hemiacetal, is much faster than the first step (figure 13).

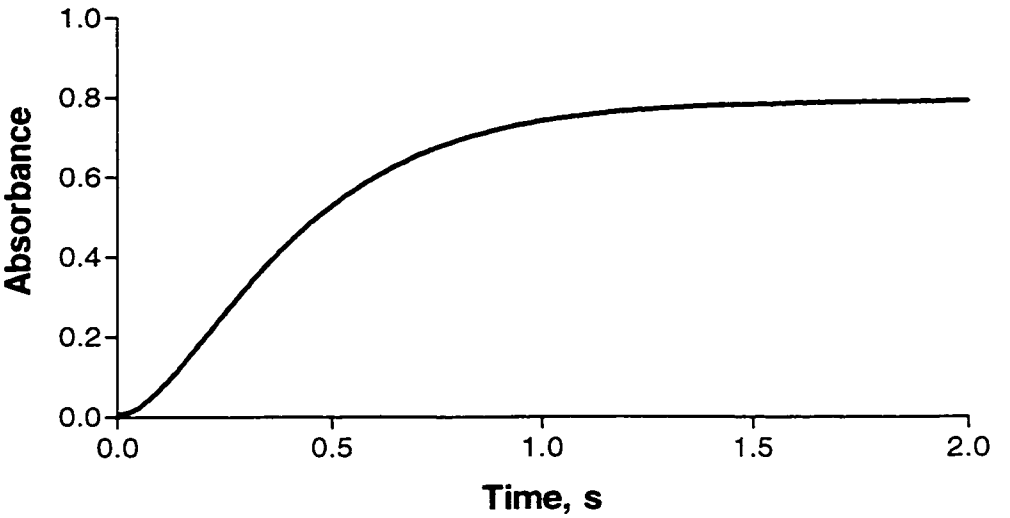

Figure 22. Example of trace for hydrolysis of acetals.

As a consequence, most of the absorbance increase is due to the rate limiting first step, and analysis of final 80-90% of trace gives the observed rate constant for this step. Values of k_{obsd} for all acetals were obtained in this manner, and all measurements were done in the chloroacetate buffer, pH=3.40, at 25±0.1°C.

Equation 15 was fitted to the k_{obsd} vs. [SDS] data observed in order to obtain the constants K_S and k_c, which are collected in table 6.

Table 6. Constants for the Hydrolysis of Acetals in Presence of SDS Micelles[a]

	k_U, s^{-1}	K_S, mM	k_C, s^{-1}
Ph-CH-$(OMe)_2$	0.0157	20.7±1.2	0.168±0.005
Ph-C(CH_3)-$(OMe)_2$	0.420	12.0±0.7	7.55±0.20
Ph-C-$(OMe)_3$	0.0395	7.81±0.47	0.929±0.020
3-Cl-Ph-CH-$(OEt)_2$	0.00414	1.31±0.20	0.0258±0.0004
4-Cl-Ph-CH-$(OEt)_2$	0.0188	1.90±0.09	0.152±0.001
Ph-CH-$(OEt)_2$	0.0528	6.38±0.51	0.612±0.015
4-Bu-Ph-CH-$(OEt)_2$	0.191	0.115±0.005	4.72±0.01
4-OMe-Ph-CH-$(OEt)_2$	0.665	5.80±0.57	27.5±0.8

a) in aqueous 0.1M chloroacetate buffer, pH=3.4, at 25 ± 0.1 °C. k_u values were obtained experimentally, K_S and k_c from fitting of the equation 15 to observed data.

Table 7. Calculated Constants for the Hydrolysis of Acetals in Presence of SDS Micelles.

	k_C/k_U	k_2, $M^{-1}s^{-1}$	K_{TS}, mM
Ph-CH-$(OMe)_2$	10.7	8.12	1.94
Ph-C(CH_3)-$(OMe)_2$	18.0	629	0.668
Ph-C-$(OMe)_3$	23.5	119	0.332
3-Cl-Ph-CH-$(OEt)_2$	6.23	19.7	0.210
4-Cl-Ph-CH-$(OEt)_2$	8.04	80.0	0.236
Ph-CH-$(OEt)_2$	11.6	95.9	0.551
4-Bu-Ph-CH-$(OEt)_2$	24.7	4.10E4	0.00465
4-OMe-Ph-CH-$(OEt)_2$	41.4	4.74E3	0.140

For both series of acetals catalysis of hydrolysis by SDS micelles was observed, and the reaction followed saturation kinetics (figures 23 and 24). The substrate binding was found to be a function of the size of substituent (table 6). From curves in figures 23 and 24 it is seen that the magnitude of catalysis depends on the nature of the substituent as well.

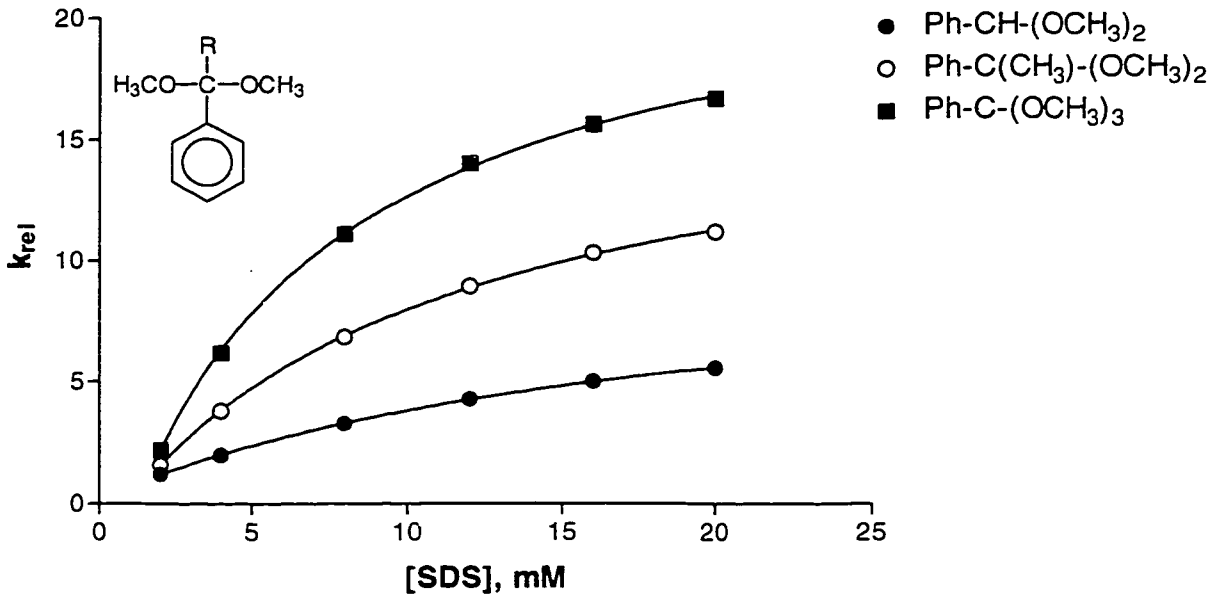

Figure 23. Dependence of Relative Rate Constant for Hydrolysis of Carbonyl Carbon Substituted Acetals on SDS Concentration.

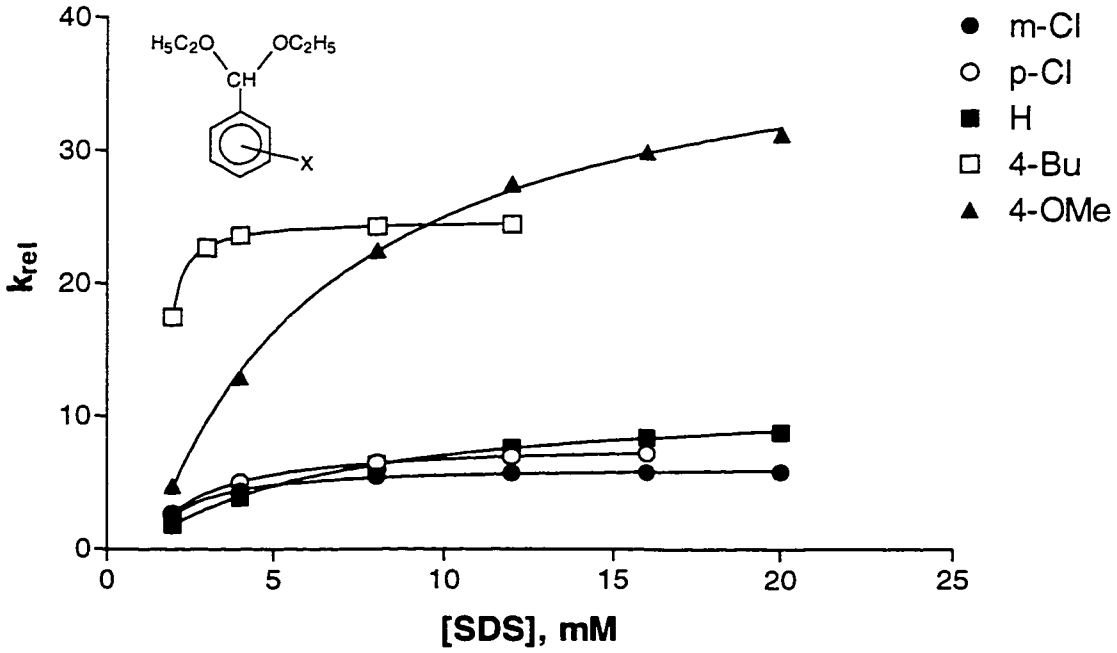

Figure 24. Dependence of Relative Rate Constant for Hydrolysis of aryl substituted acetals on SDS concentration

Discussion.

The derived parameters k_c/k_u, k_2, and K_{TS} were calculated for this reaction for all acetals and are summarized in the table 7.

Since the transition state for the reaction of acetal hydrolysis is essentially a positively charged carboxonium ion, the nature of the substituent should affect the reactivity of the substrate. For the carbonyl carbon substituted series, acetophenonedimethyl acetal ($PhCMe(OMe)_2$) is more reactive than parent compound ($PhCH(OMe)_2$), since the methyl group is electron-donating, which stabilizes the transition state. On the other hand, trimethyl orthobenzoate is only slightly more reactive than benzaldehyde dimethyl acetal, because electron-withdrawing power of oxygen almost compensates for the stabilization of the transition state by an electron pair of the methoxy group.

In the aryl substituted series, all electronic effects of substituents are applied through the π-system of benzene ring. Introduction of electron-withdrawing chlorine atoms in *meta*- and *para*- positions leads to reduced reactivity of these compounds in comparison with the parent benzaldehyde diethyl acetal. Also, chlorine in *meta*-position has greater effect than in *para*- position, since it is closer to the reaction centre and it is less electron-releasing. Electron-donating butyl group in *para*-position increases the reactivity of the acetal. As opposed to trimethyl orthobenzoate, in *p*-methoxybenzaldehyde diethyl acetal the inductive effect of the methoxy group is eliminated by distance, and stabilisation of TS by an electron pair

through conjugation plays the leading role. This leads to the fact that *p*-methoxybenzaldehyde diethyl acetal is the most reactive acetal of all those studied in the present work.

For the micelle assisted hydrolysis the binding of acetals to micelles depends clearly on the size of substituent and increases in sequence R=H < Me < OMe. The maximum acceleration k_c/k_u increases in the same direction. This is understandable, since plot of pK_S vs. pK_{TS} (figure 25) is a straight line with a slope of 1.81± 0.09. The linearity of the plot suggests that same factors are responsible for binding of both substrate and TS to the micelle, and the slope greater than one indicates that binding of TS is more sensitive towards changes in acetal structure. The situation is different, however, with aryl substituted acetal, where the correlation between pK_S and pK_{TS} is not particularly linear (figure 26).

In general, the same trend is seen for both pK_S and pK_{TS}: the larger the substituent, the stronger binding of the substrate and of TS to the micelle. However, the TS becomes more sensitive to the electronic nature of the substituent in the micellar media, and so it looks like the TS binding is more sensitive than substrate binding to the structural changes for electron-donating substituents, and less sensitive for electron-withdrawing. The maximum acceleration k_c/k_u increases markedly with the increase in the electron-donating ability of the substituent.

Quantitatively, these trends can be estimated using a Hammett plot. In figure 27 two Hammett plots for the hydrolysis of aryl substituted series of acetals are presented. Both k_u, the rate constant in absence of SDS, and k_c, the theoretical limit for the accelerated rate constant at complete saturation, are related to σ values for

the respective substituent. The slopes of the Hammett plots are ρ, the reaction constant. In the case of k_u, ρ=-3.19 ± 0.27, whereas ρ=-4.44 ± 0.40 for k_c. Since ρ can be considered as a measure of susceptibility of a reaction to the electron-donating or electron-withdrawing effect of a substituent[67], it is possible to conclude that TS develops much farther (has more positive character) when the reaction is assisted with micelles.

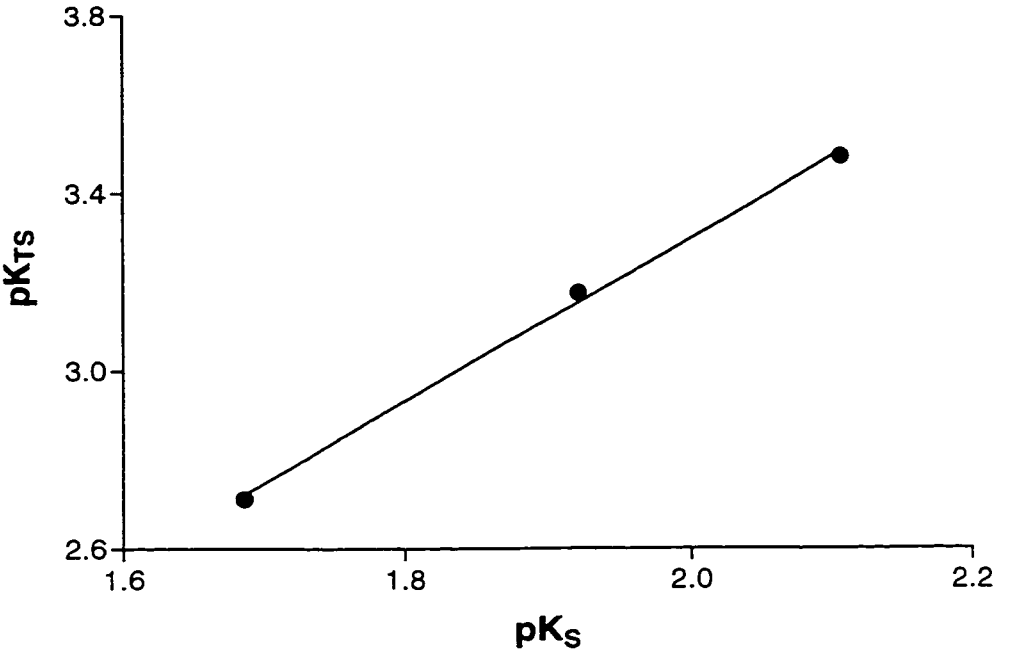

Figure 25. Correlation Between Substrate and Transition State Binding to SDS for the Hydrolysis of Carbonyl Carbon Substituted Acetals.

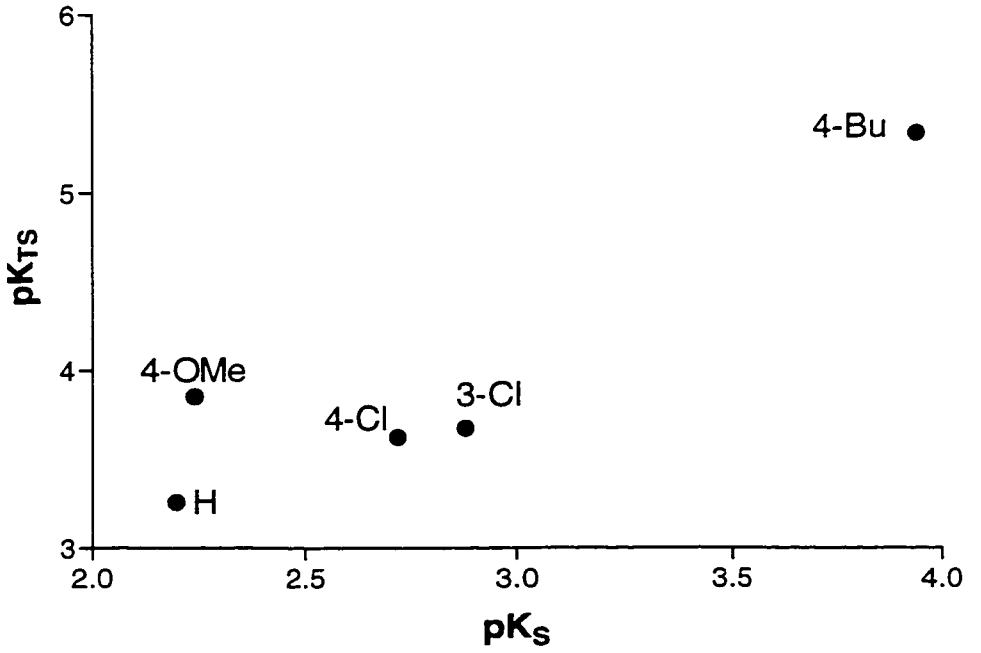

Figure 26. Correlation Between Substrate and Transition State Binding to SDS for the Hydrolysis of Aryl Substituted Acetals.

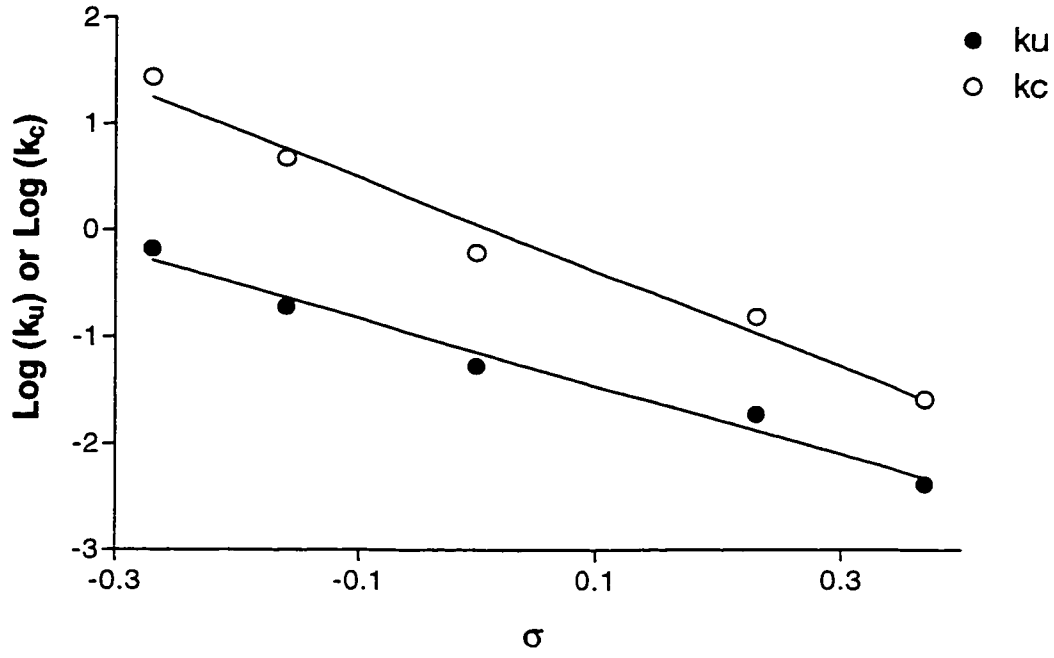

Figure 27. The Hammett Plot for the Hydrolysis of Aryl Substituted Acetals.

Reactions Mediated by Dendrimers.

Cleavage of *p*-Nitrophenyl Alkanoates.

Since the idea was to investigate the stabilisation of transition states of reactions by dendrimers, a novel class of macromolecular compounds, and maybe, to make some comparisons between dendrimers and micelles, systematic studies on the cleavage of *p*-nitrophenyl alkanoates by dendrimers were performed. Dendrimers from the family of so-called Starburst (PAMAM) were used. These dendrimers have two subfamilies: amino-terminated dendrimers (integer generations), and carboxyl-terminated dendrimers (half-generations). General structure and descriptions of the core, repeat units, and surface groups are given on the figure 28.

Kinetic measurements have been made on cleavage of *p*-nitrophenyl alkanoates in the presence of four generations of amino-terminated dendrimers and three generations of carboxyl-terminated dendrimers (figure 28). They were performed in the manner similar to experiments with micelles. Equation 2 was used to analyse the data, and measured and fitted values are collected in the table 8 for the amino-terminated dendrimers and in the table 9 for the carboxyl-terminated dendrimers. The raw data are collected in Appendix 3.

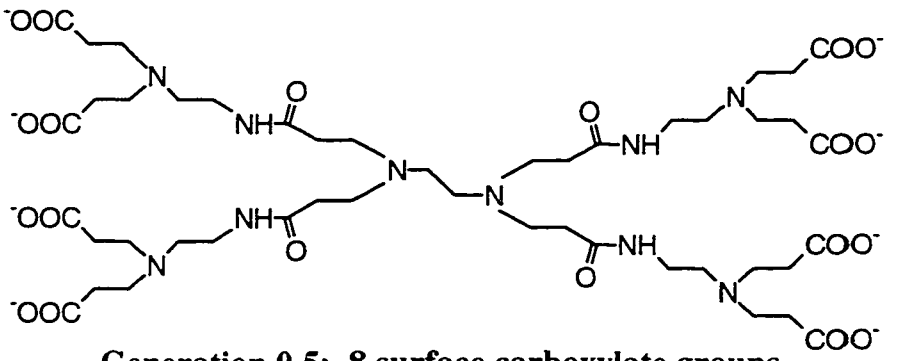

Generation 0.5: 8 surface carboxylate groups

Generation 1.5: 16 surface carboxylate groups

Generation 2.5: 32 surface carboxylate groups

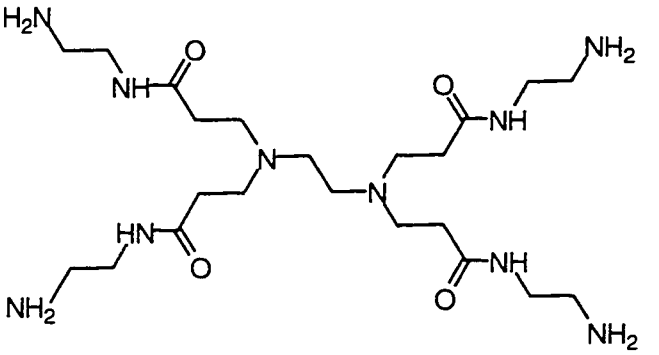

Generation 0: 4 surface amino groups

Generation 1: 8 surface amino groups

Generation 2: 16 surface amino groups

Generation 3: 32 surface amino groups

Initiator Core: 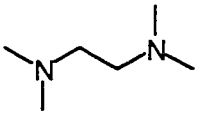

Repeat unit: 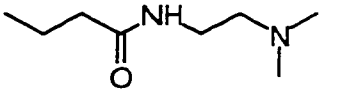

Figure 28. Amino-terminated and Carboxyl-terminated polyamidoamine (PAMAM) Dendrimers: General Structure, Core, Surface and Repeat Units.

Amino-terminated dendrimers were found to catalyse the cleavage of *p*-nitrophenyl alkanoates, which is not surprising. For all esters and all dendrimer generations saturation behaviour was observed (figures 29 and 30). Binding of a substrate to dendrimers depends on a generation number, which is reflected in a degree of curvature of plots k_{rel} vs. [Dendrimer]. Inside the particular generation the dependence of substrate binding on acyl chain length is not so expressed, except, maybe, for the dendrimer of generation 3.

Much more surprising were results obtained with carboxyl-terminated dendrimers, which were proposed to serve as unimolecular models of anionic micelles[37,38]. Opposite to the micellar behaviour, these dendrimers also *catalyse* cleavage of *p*-nitrophenyl alkanoates under reaction conditions. Saturation kinetics was observed in this case as well, and the dependence of relative rate constants on the dendrimer concentration is shown in figures 31 and 32.

Measurements were performed at two pH's: 10.6 in carbonate buffer and 11.6 in phosphate buffer. Initial rate constants were approximately 10 times less at lower pH, which reflects decrease in concentration of attacking nucleophile (OH^-) by the same factor. The determined strength of substrate binding increased with growth of the dendrimer size, moreover it also increased when the pH of the solution was lower for each of the esters and for all dendrimers studied. As for amino-terminated dendrimers, the dependence of K_S on the acyl chain length was not large.

Table 8. Constants for the Cleavage of *p*-Nitrophenyl Alkanoates in Presence of Amino-terminated Dendrimers[a].

	k_U, s^{-1}	K_S, mM	k_C, s^{-1}
Dendrimer 0			
C_2	0.0651	47.9±4.1	0.651±0.043
C_3	0.0649	61.6±4.2	0.675±0.037
C_4	0.0407	50.9±10.7	0.344±0.008
C_5	0.0418	51.1±7.1	0.398±0.043
C_6	0.0376	30.0±4.5	0.237±0.025
C_7	0.0394	43.1±5.7	0.303±0.029
C_8	0.0358	32.3±4.7	0.253±0.026
Dendrimer 1			
C_2	0.0861	24.3±2.1	0.970±0.050
C_3	0.0914	18.3±1.2	0.750±0.031
C_4	0.0577	15.4±2.2	0.391±0.032
C_5	0.0492	16.6±0.8	0.417±0.013
C_6	0.0480	13.5±1.6	0.354±0.028
C_7	0.0286	13.2±2.2	0.320±0.030
C_8	0.0352	12.8±1.9	0.296±0.024

(Continued...)

Dendrimer 2

C_2	0.0999	14.7±0.6	1.56±0.05
C_3	0.0973	14.0±2.0	0.987±0.098
C_4	0.0428	10.3±2.1	0.516±0.074
C_5	0.0436	6.19±0.51	0.333±0.015
C_6	0.0354	5.40±0.77	0.311±0.026
C_7	0.0364	5.00±0.82	0.271±0.023
C_8	0.0352	4.41±0.44	0.229±0.011

Dendrimer 3

C_2	0.0741	4.28±0.12	0.965±0.017
C_3	0.0650	3.27±0.36	0.543±0.035
C_4	0.0417	2.92±0.27	0.320±0.016
C_5	0.0401	2.58±0.23	0.310±0.015
C_6	0.0391	2.10±0.20	0.240±0.011
C_7	0.0445	2.01±0.22	0.246±0.012
C_8	0.0461	0.859±0.054	0.138±0.005

a) in aqueous 0.2M phosphate buffer, pH=11.6, at 25 ± 0.1 °C. k_u values were obtained experimentally, K_S and k_c from fitting of equation 2 to observed data.

Table 9. Constants for the Cleavage of *p*-Nitrophenyl Alkanoates in Presence of Carboxyl-terminated Dendrimers[a].

	k_U, s^{-1}	K_S, mM	k_C, s^{-1}
Dendrimer 0.5			
pH=11.6			
C_2	0.0701	139±23.1	2.26±0.34
C_4	0.0427	49.1±4.4	0.532±0.037
C_6	0.0407	43.2±2.8	0.491±0.025
pH=10.6			
C_2	0.00818	21.9±2.3	0.0398±0.0020
C_4	0.00490	21.9±6.0	0.0215±0.0030
C_6	0.00643	15.5±2.7	0.0247±0.0020
Dendrimer 1.5			
pH=11.6			
C_2	0.0635	22.4±4.5	0.779±0.121
C_4	0.0382	12.6±2.0	0.290±0.030
C_6	0.0374	11.6±3.8	0.282±0.060
pH=10.6			
C_2	0.00789	7.86±2.48	0.0326±0.0060
C_4	0.00305	4.31±0.42	0.00949±0.00030
C_6	0.00290	3.69±0.52	0.00832±0.00040

(Continued...)

Dendrimer 2.5

	pH=11.6		
C_2	0.1006	7.18±0.79	0.848±0.065
C_4	0.0630	6.06±1.25	0.438±0.061
C_6	0.0510	4.83±0.79	0.387±0.037
	pH=10.6		
C_2	0.0105	5.16±0.79	0.0530±0.0050
C_4	0.00625	2.87±0.51	0.0202±0.0015
C_6	0.00556	1.67±0.21	0.0158±0.0007

a) in aqueous 0.2M phosphate buffer for pH=11.6, or in aqueous carbonate buffer for pH=10.6 at 25 ± 0.1 °C. k_u values were obtained experimentally, K_S and k_c from fitting of equation 2 to observed data.

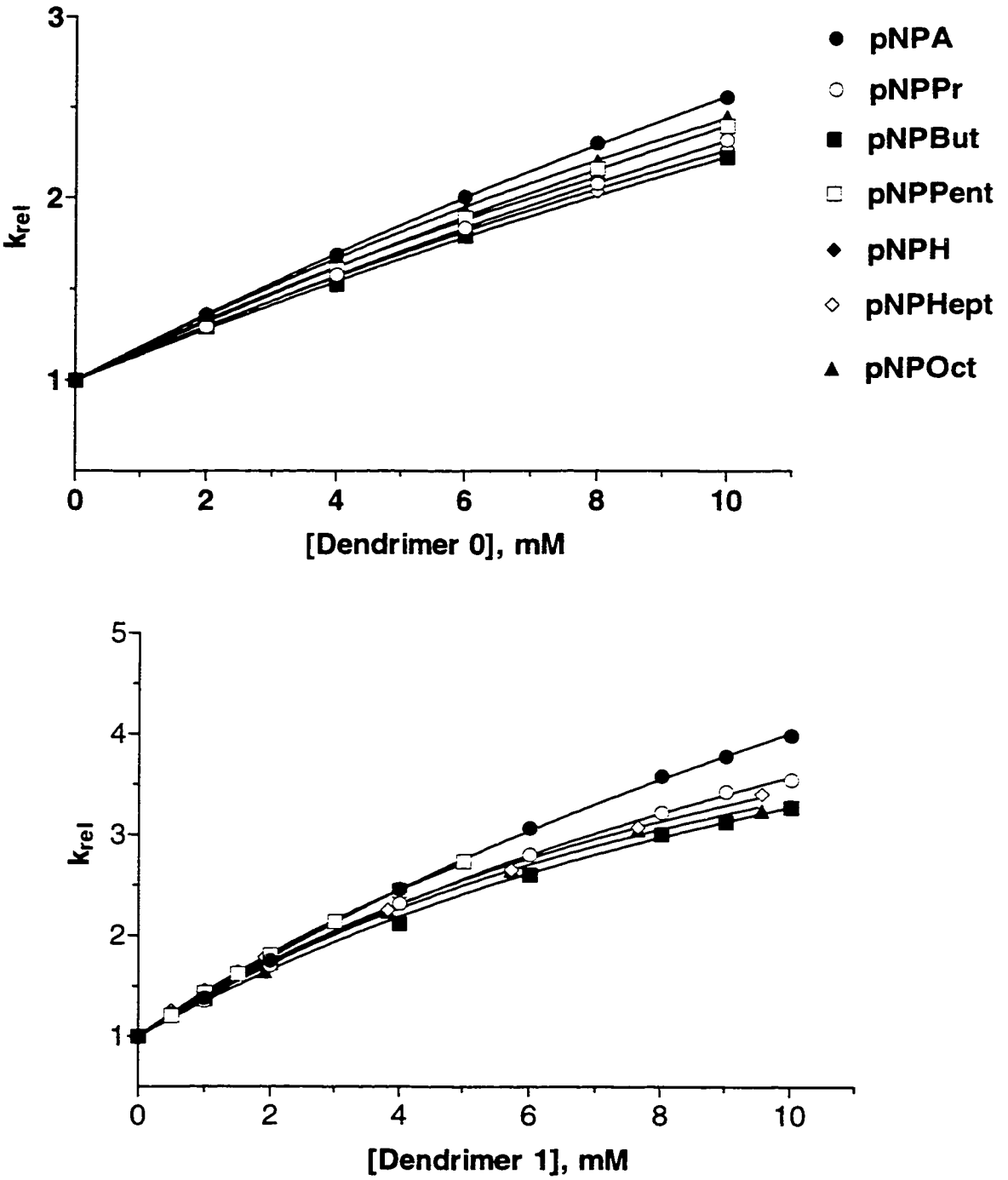

Figure 29. Dependence of Relative Rate Constant for Cleavage of *p*-Nitrophenyl Alkanoates on Dendrimer 0 and Dendrimer 1 Concentration.

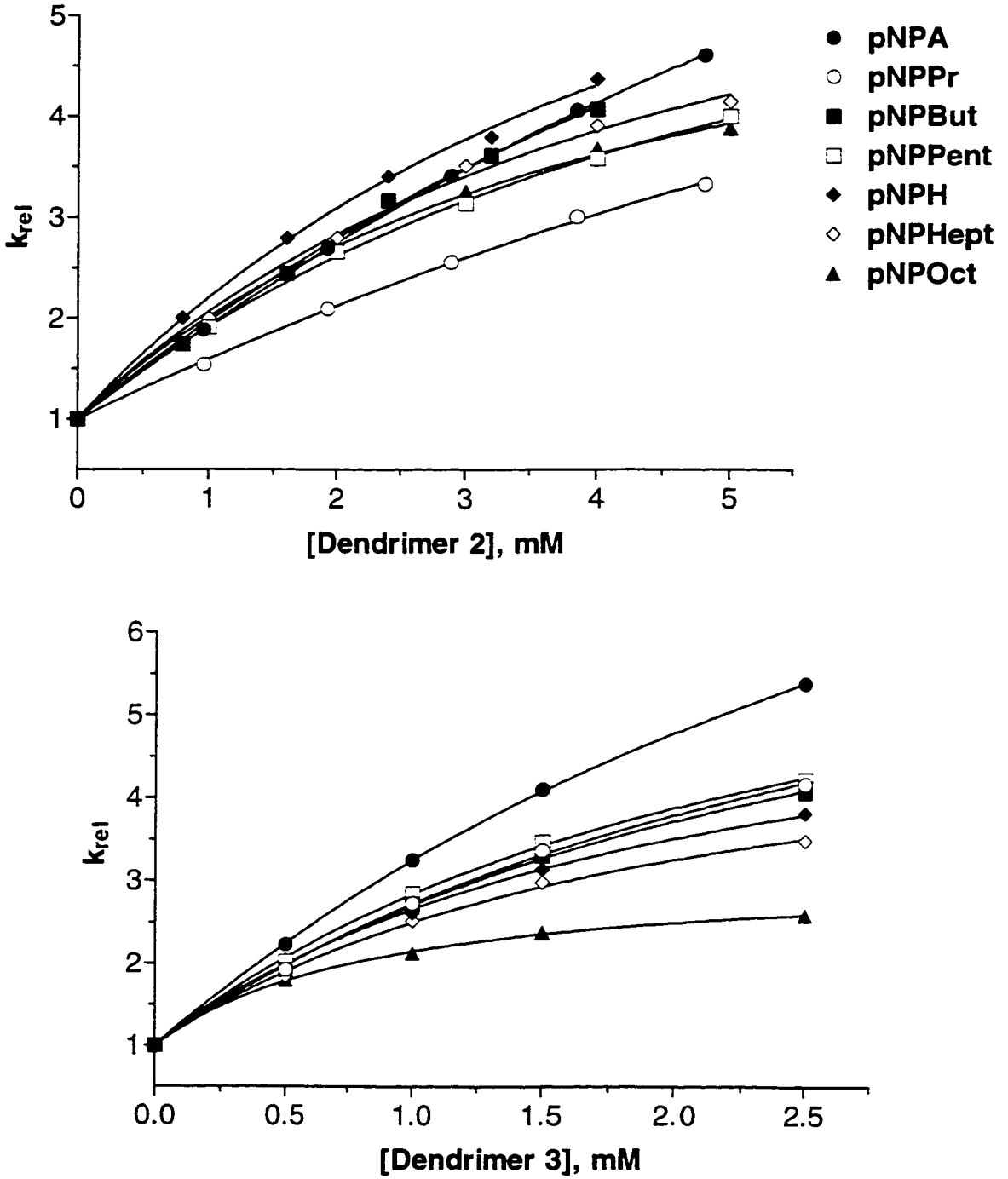

Figure 30. Dependence of Relative Rate Constant for Cleavage of *p*-Nitrophenyl Alkanoates on Dendrimer 2 and Dendrimer 3 Concentration.

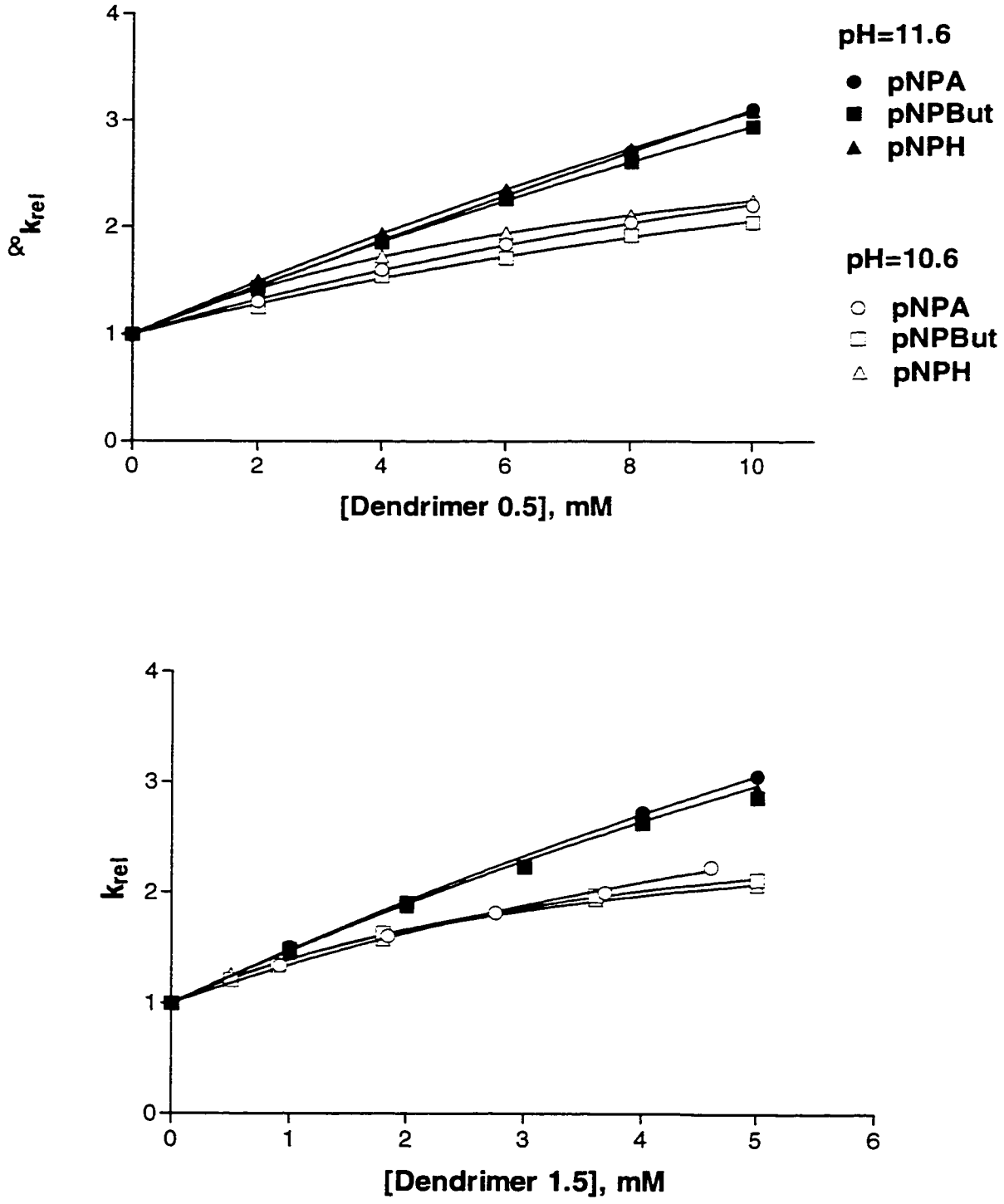

Figure 31. Dependence of Relative Rate Constant for Cleavage of *p*-Nitrophenyl Alkanoates on Dendrimer 0.5 and Dendrimer 1.5 Concentration.

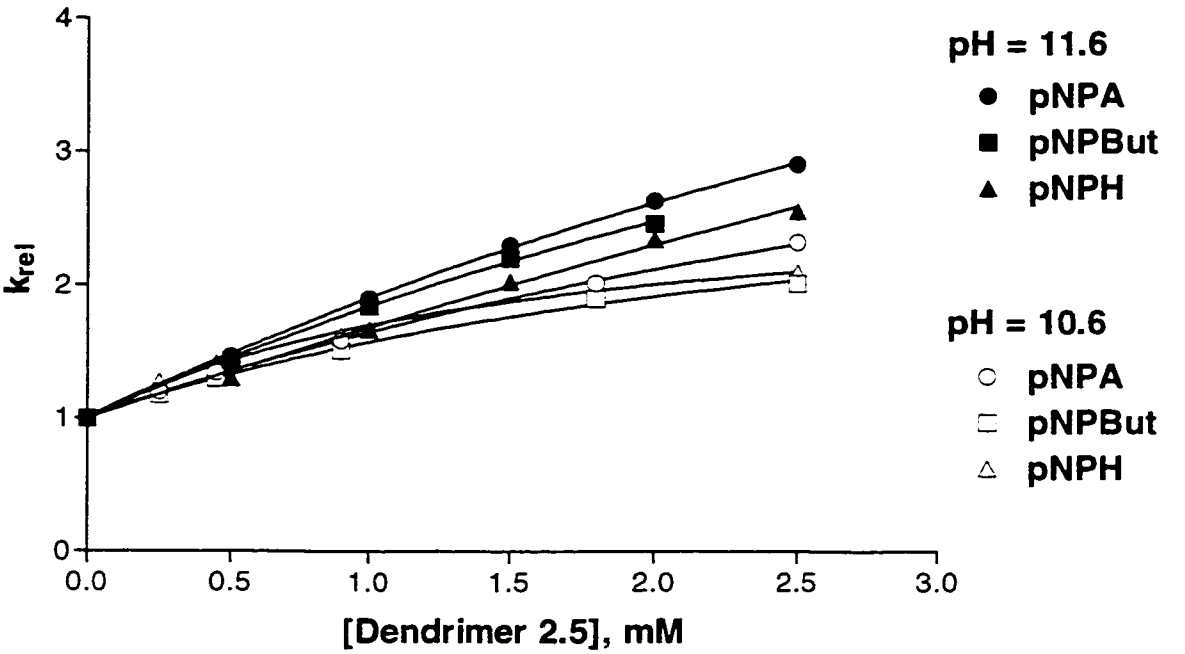

Figure 32. Dependence of Relative Rate Constant for Cleavage of *p*-Nitrophenyl Alkanoates on Dendrimer 2.5 Concentration.

Discussion.

The parameters k_c/k_u, k_2, and pK_{TS} were determined for all dendrimers and can be found in tables 10 and 11. As it has already been mentioned, the substrate binding increases with increase in generation of dendrimer number, and exhibits very small dependence on the acyl chain length, only slightly increasing as chain growth. The binding of transition state behaves in the similar manner: higher generations of dendrimers stabilize the transition state much more effectively than lower ones, but the dependence of TS binding on the acyl chain length for each dendrimer generation is almost absent. This lack of dependence of both substrate and TS binding on the acyl chain length is seen very well in figures 33 and 34, where pK_S and pK_{TS} are plotted against the number of carbons in the acyl group. In both cases and for all dendrimers plots are essentially parallel to the *X* axis.

If PAMAM dendrimers are compared with micelles, a very important distinction must be noted: the area of dendrimer which is between surface groups and inner core is *not* hydrophobic. Not only hydrophobic interaction, but other types, like electrostatic and Van der Waals forces, all take part in the process of binding the substrate. Varying only the chain length of the substrate means changing mainly the hydrophobic component, and this explains why the dependence on the acyl chain length is virtually absent.

Table 10. Calculated Constants for the Cleavage of *p*-Nitrophenyl Alkanoates in Presence of Amino-terminated Dendrimers.

	k_C/k_U	k_2, $M^{-1}s^{-1}$	K_{TS}, mM
Dendrimer 0			
C_2	10.0	13.6	4.79
C_3	10.4	11.0	5.92
C_4	8.45	6.76	6.02
C_5	9.52	7.79	5.37
C_6	6.30	7.90	4.76
C_7	7.69	7.03	5.60
C_8	7.07	7.83	4.57
Dendrimer 1			
C_2	11.3	39.9	2.16
C_3	8.21	41.0	2.23
C_4	6.78	25.4	2.27
C_5	7.20	25.1	1.96
C_6	6.67	26.2	1.83
C_7	10.3	24.2	1.18
C_8	8.41	23.1	1.52

(Continued...)

Dendrimer 2

C_2	15.6	106	0.941
C_3	10.1	70.5	1.38
C_4	12.1	50.1	0.854
C_5	7.64	53.8	0.810
C_6	8.79	57.6	0.615
C_7	7.45	54.2	0.672
C_8	6.59	52.6	0.669

Dendrimer 3

C_2	12.9	223	0.332
C_3	8.35	166	0.391
C_4	7.67	110	0.381
C_5	7.73	120	0.334
C_6	6.14	114	0.342
C_7	5.53	122	0.364
C_8	2.99	161	0.287

Table 11. Calculated Constants for the Cleavage of *p*-Nitrophenyl Alkanoates in Presence of Carboxyl-terminated Dendrimers.

	k_C/k_U	k_2, $M^{-1}s^{-1}$	K_{TS}, mM
Dendrimer 0.5			
pH=11.6			
C_2	32.2	16.2	4.32
C_4	12.5	10.8	3.93
C_6	12.1	11.4	3.57
pH=10.6			
C_2	4.87	1.82	4.51
C_4	4.33	0.980	4.99
C_6	3.15	1.59	4.93
Dendrimer 1.5			
pH=11.6			
C_2	12.3	34.8	1.83
C_4	7.60	23.0	1.66
C_6	7.54	24.3	1.54
pH=10.6			
C_2	4.13	4.15	1.90
C_4	3.11	2.20	1.39
C_6	2.87	2.25	1.29

(Continued...)

Dendrimer 2.5

	pH=11.6		
C_2	8.43	118	0.852
C_4	6.96	72.3	0.871
C_6	7.58	80.2	0.640
	pH=10.6		
C_2	5.04	10.3	1.02
C_4	3.23	7.02	0.890
C_6	2.84	9.47	0.590

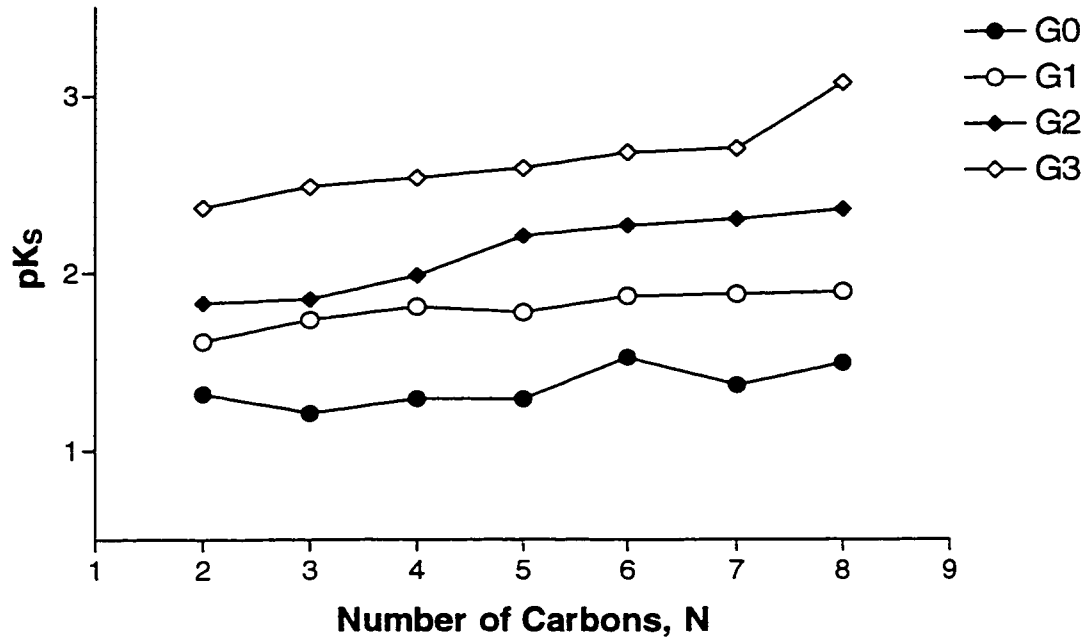

Figure 33. Acyl Chain Length Dependence of the Substrate Binding (pK_S) for the Cleavage of *p*-Nitrophenyl Alkanoates in Presence of Amino-terminated Dendrimers.

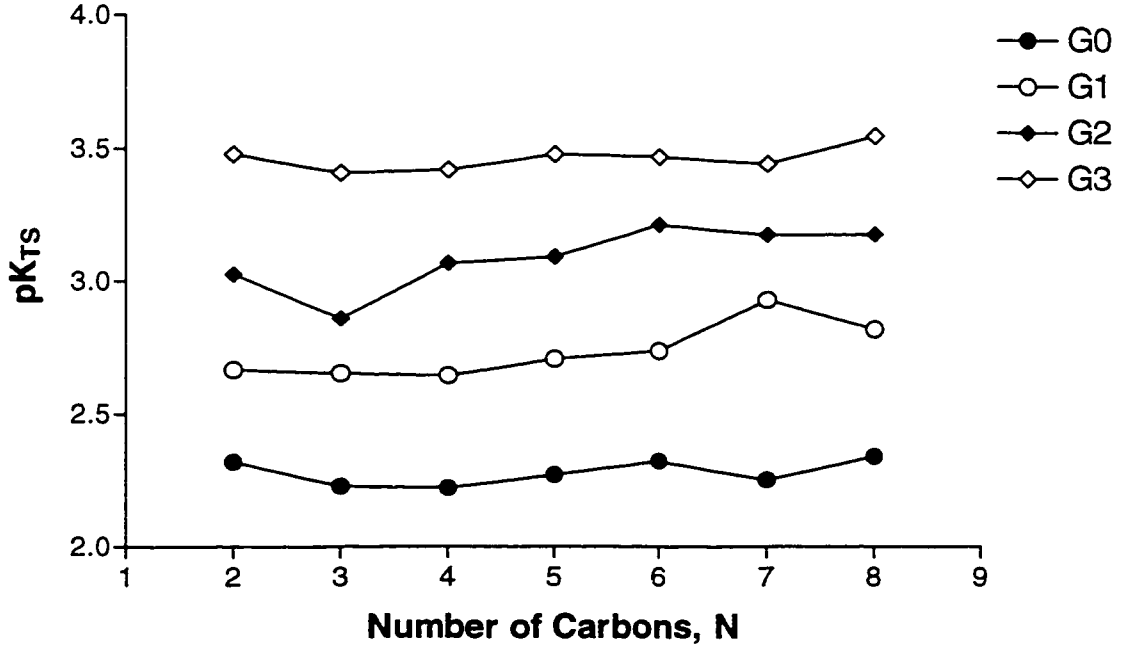

Figure 34. Acyl Chain Length Dependence of Transition State Stabilization (pK_{TS}) for the Cleavage of *p*-Nitrophenyl Alkanoates in Presence of Amino-terminated Dendrimers.

However, moving from generation to generation, the number of different sites for *all* possible interactions increases, which leads to increase in substrate binding and the degree of TS stabilization. But the dependence of TS stabilization, as well as of k_2, the apparent second order rate constant for the reaction between substrate and catalyst (equation 8), on the dendrimer generation has an interesting feature of its own.

Since the amino group is a good nucleophile, we made a suggestion that in case of amino-terminated dendrimers the process is not a pure catalysis, but rather the reaction of aminolysis. Thus, the second order rate constant should be proportional to the number of terminal amino groups $\boldsymbol{T}$ (equation 16):

$$k_2 = a * T \qquad (16).$$

But according to equation 4, for the dendrimer with $N_C = 4$, and $N_R = 2$, the number of terminal groups related to the dendrimer generation number $\boldsymbol{n}$ as follows:

$$T = 2^{n+2} \qquad (17).$$

Substituting the expression for $\boldsymbol{T}$ to the (16) and taking logarithms, we have:

$$Log(k_2) = Log(a) + (n+2) * Log2 \approx const + 0.3 * n \qquad (18).$$

Thus, plot of Log (k_2) vs. generation number should be a straight line with a slope of 0.3. Similarly, it can be shown that plot of pK_{TS} vs. generation number should have the same properties. Such plots are shown in figures 35 and 36.
All slopes of the plots in this figures are between 0.37 and 0.42, and this leads to a conclusion that not only the surface of the dendrimers are responsible for the chemistry of the process, but also internal parts are making certain contribution.

The results on cleavage of *p*-nitrophenyl alkanoates in presence of carboxylate-terminated dendrimers presents a situation, that is even more complicated. Since carboxyl group can not be considered as strong nucleophile as amino group, it is hard to expect the involvement of these carboxyls in direct attack on the carbonyl carbon of the ester. Nevertheless, the magnitude of acceleration (*ca.* 8-12 times) is comparable with reactions carried out in presence of amino-terminated dendrimers at pH=11.6. If data for two subfamilies of dendrimers with the same number of surface groups are compared, it is seen that the second order rate constant k_2 is only 2 times or less higher for the amino-terminated dendrimers as compared to their carboxylate analogues. The relation between TS binding is approximately the same for two dendrimer subfamilies. Another interesting feature is that slopes for the plots of k_2 and pK_{TS} vs. Generation number are very similar to ones obtained for the reaction in presence of amino-terminated dendrimers - 0.34-0.44 (figures 37 and 38).

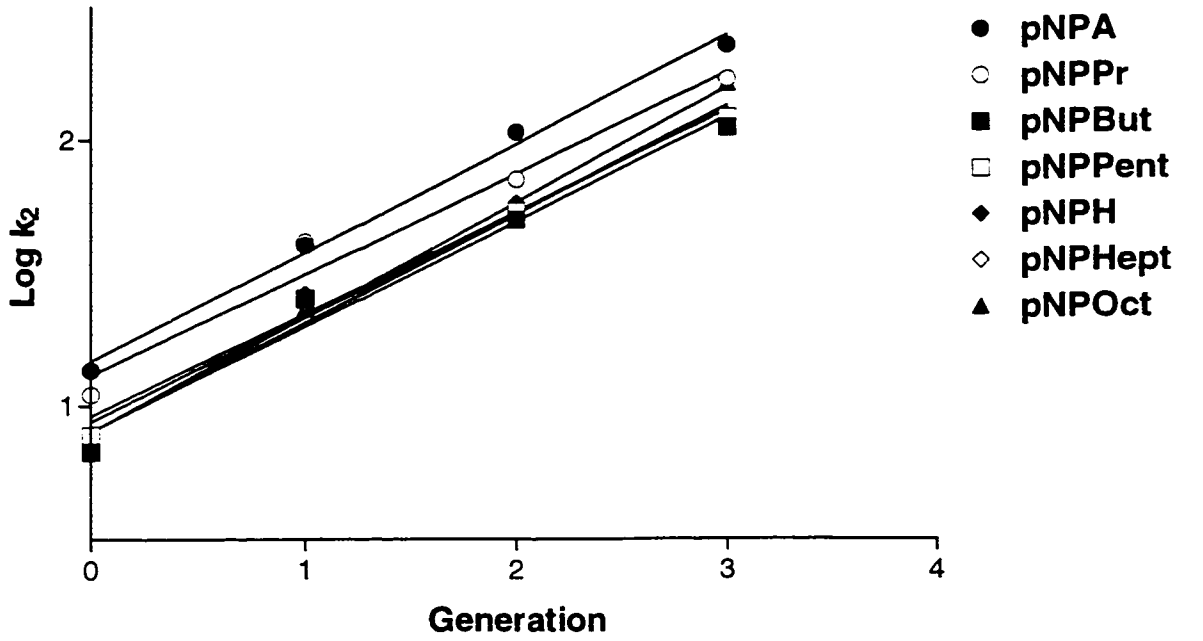

Figure 35. Plot of the Second Order Rate Constant k_2 vs. Generation Number for the Reaction of Cleavage of *p*-Nitrophenyl Alkanoates in Presence of Amino-terminated Dendrimers.

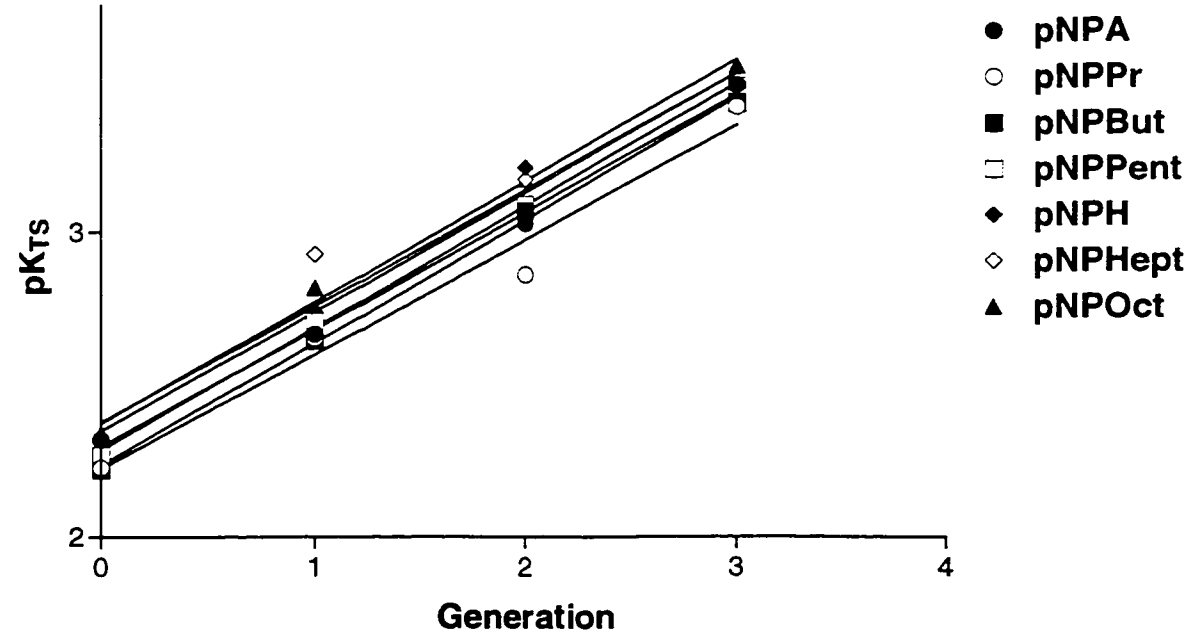

Figure 36. Plot of the Transition State Stabilization K_{TS} vs. Generation Number for the Reaction of Cleavage of *p*-Nitrophenyl Alkanoates in Presence of Amino-terminated Dendrimers.

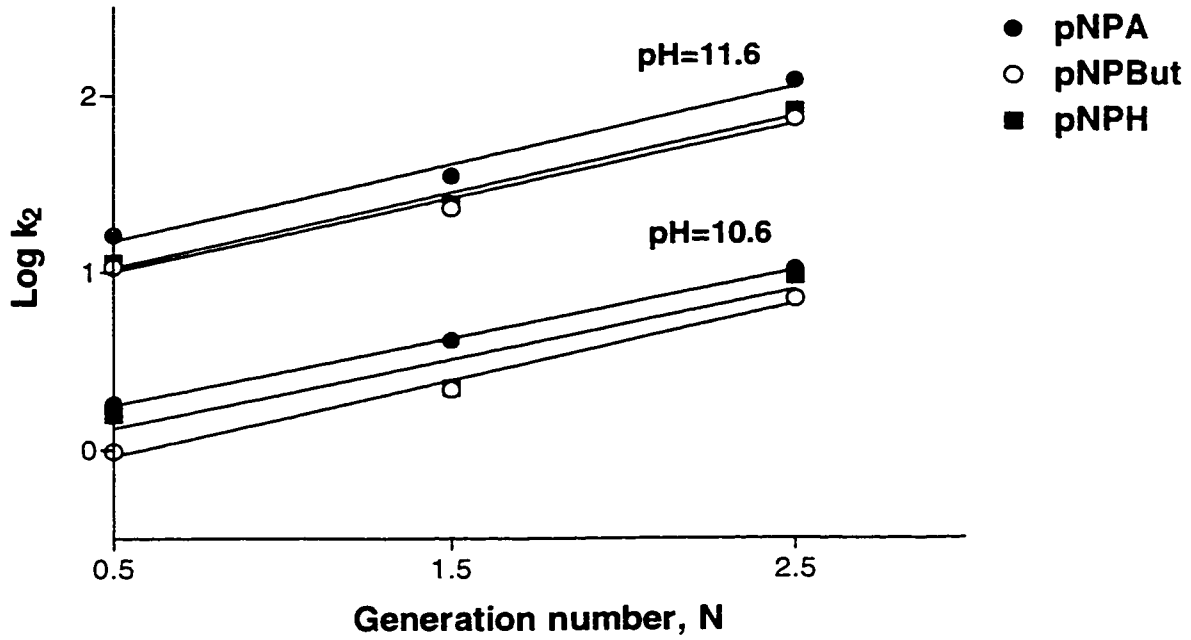

Figure 37. Plot of the Second Order Rate Constant k_2 vs. Generation Number for the Reaction of Cleavage of *p*-Nitrophenyl Alkanoates in Presence of Carboxyl-terminated Dendrimers.

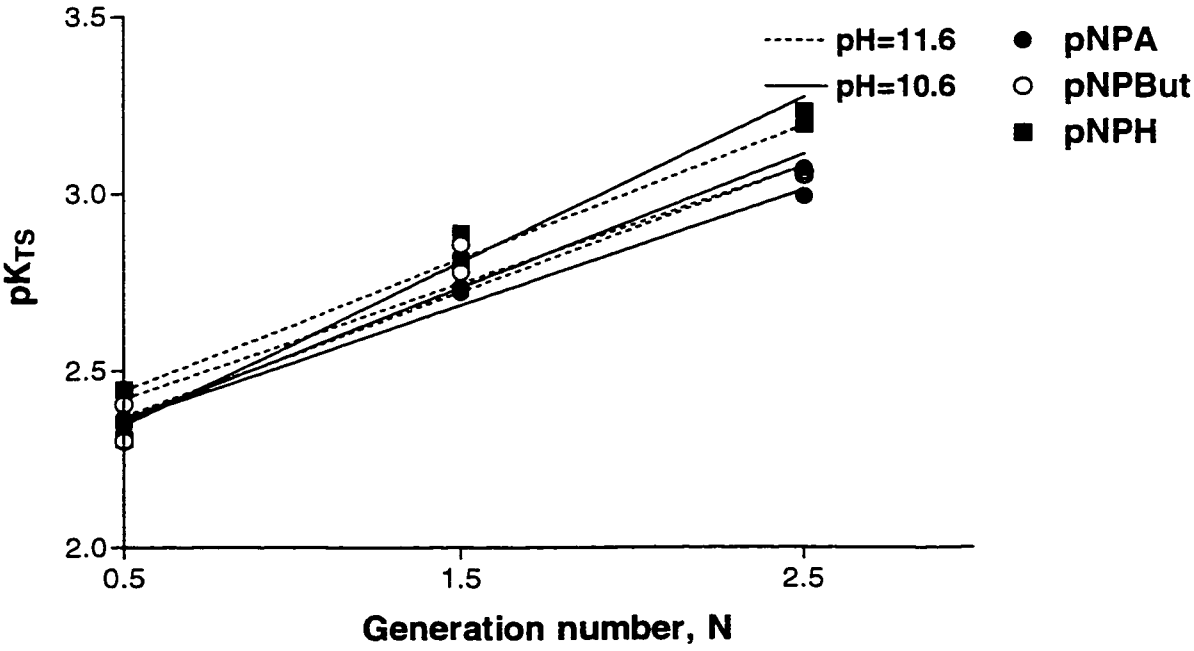

Figure 38. Plot of the Transition State Stabilization K_{TS} vs. Generation Number for the Reaction of Cleavage of *p*-Nitrophenyl Alkanoates in Presence of Carboxyl-terminated Dendrimers.

Even though the surface group type was changed the sensitivity of the reaction towards the dendrimers left more or less the same, which again leads to a conclusion about strong involvement of internal parts of dendrimers. There was an idea that it was internal tertiary nitrogens of dendrimers which made a significant contribution to the catalysis. To test this hypothesis experiments were performed on cleavage of *p*-nitrophenyl acetate, and *p*-nitrophenyl butanoate in presence of 3,3',3"-nitrilotripropionic acid (structure is shown in figure 39). This acid resembles a fragment of carboxyl-terminated dendrimer, and we hoped it would give us some insights to the catalysis process.

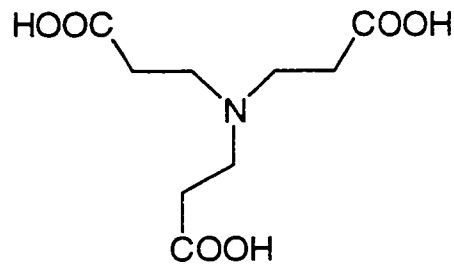

Figure 39. Structure of 3,3',3"-Nitrilotripropionic Acid.

As it turned out, the rate of reaction was found to be almost independent of the concentration of the acid. There was no evidence of saturation behaviour, since dependence of observed rate constant on acid concentration (figure 40) is a straight line in both cases, with slopes correspond to a second order rate constant k_2 of the reaction 1.04 ± 0.1 and 0.774 ± 0.046 $M^{-1}s^{-1}$ for pNPA and pNPBut, respectively.

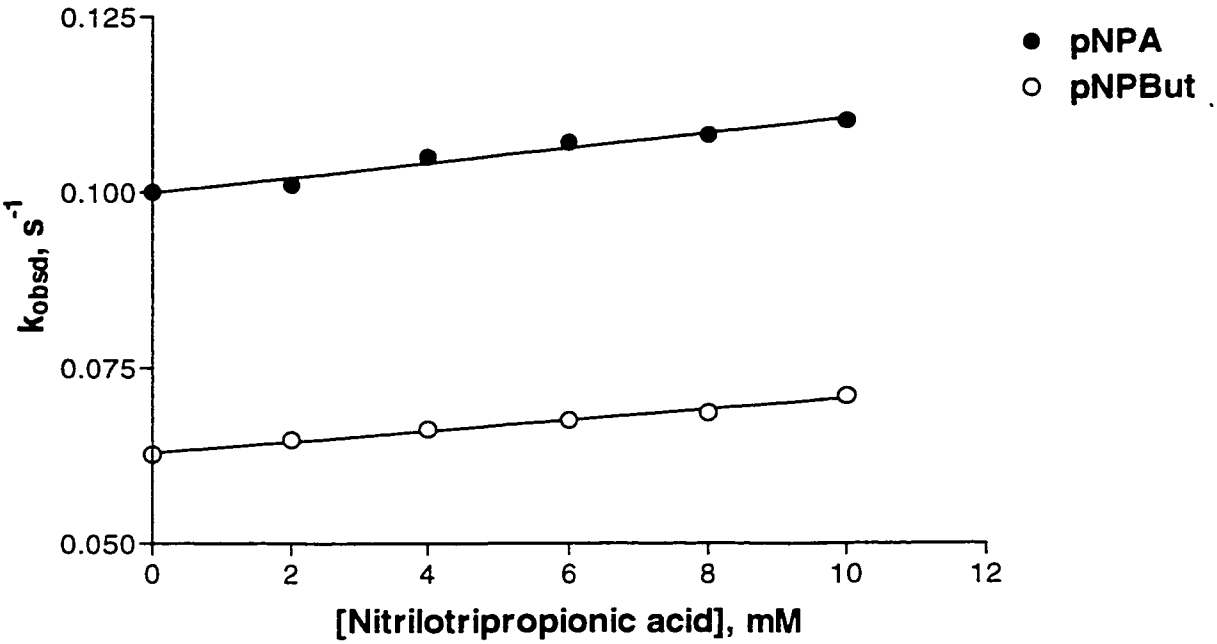

Figure 40. Dependence of Observed Rate Constant on the Concentration of 3,3',3"-Nitrilotripropionic Acid for the Cleavage of *p*-Nitrophenyl Alkanoates at pH=11.6.

In the work of Evans *et al* [68]., where a similar reaction was studied, the possibility of involvement of amido-fragments was suggested (figure 48), which stabilize the formation of TS by hydrogen bonding.

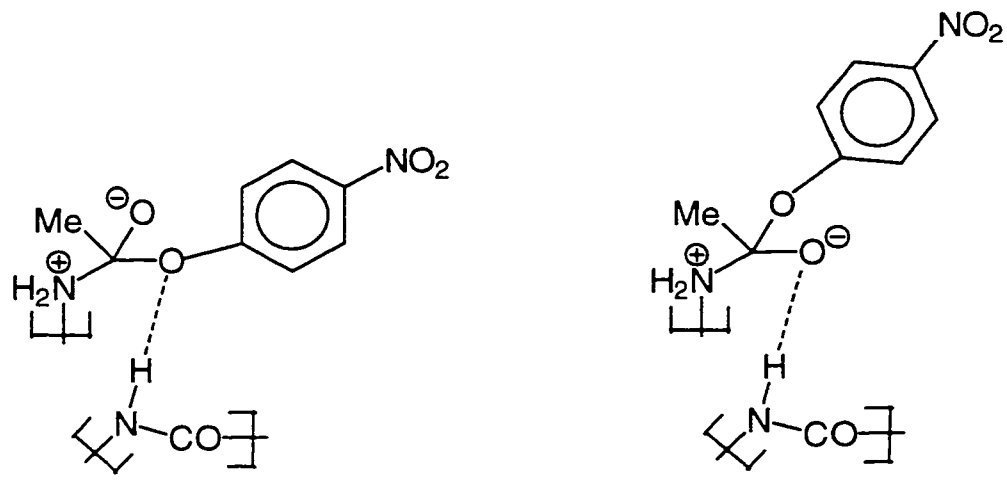

Figure 41. Possible Pathways of TS stabilization by Amino-terminated Dendrimers.

Thus the only conclusion it possible to make so far that catalysis by dendrimers is a complex *cooperative* process, involving different parts of the molecule and different forces operating through the whole system.

Hydrolysis of Acetals.

Results and Discussion.

We also studied the cleavage of acetals in presence of carboxyl-terminated dendrimers. The kinetic analysis was performed in a way similar to the one involving studies of acetal hydrolyses in presence of micelles. The series of carbonyl carbon substituted acetals was studied, and the raw data are collected in the Appendix 4. The observed and fitted constants for the reaction are collected in the table 12, and calculated constants k_c/k_u, k_2, and K_{TS} are in table 13.

Carboxyl-terminated dendrimers were found to catalyse the acidic cleavage of acetals, and reaction has saturation kinetics character for all dendrimers and acetals studied (figures 42 and 43). However, the catalysis afforded by dendrimers in these cases is rather modest, as k_c/k_u varies in a range between 1.1 and 2.4 for all substrates, and it is not changing appreciably as dendrimer becomes larger. Once again, it is a consequence of the fact, that changes in both transition state and substrate binding are parallel from generation to generation for a particular substrate.

Comparison of TS and substrate binding shows an interesting feature: while both parameters increase with generation number for trimethyl orthobenzoate, they *decrease* in the same direction for benzaldehyde dimethyl acetal and acetophenone dimethyl acetal. The different nature of these substituents can account for the observed tendency. While former has some hydrophilic character, two latter are

relatively hydrophobic. With increase in dendrimer generation the number of hydrophilic sites increases as well (since interior of PAMAM dendrimers is considered to be relatively hydrophilic), which, in turn, makes dendrimer affinity towards -OMe substituted acetal higher.

Table 12. Constants for the Hydrolysis of Carbonyl Carbon Substituted Acetals in Presence of Carboxyl-terminated Dendrimers[a].

	k_U, s^{-1}	K_S, mM	k_C, s^{-1}
Dendrimer 0.5			
Ph-CH-$(OMe)_2$	0.0176	2.97±0.61	0.0200±0.0001
Ph-C(CH_3)-$(OMe)_2$	0.372	2.37±0.07	0.547±0.001
Ph-C-$(OMe)_3$	0.0373	10.6±1.1	0.0640±0.0020
Dendrimer 1.5			
Ph-CH-$(OMe)_2$	0.0141	3.57±0.91	0.0191±0.0006
Ph-C(CH_3)-$(OMe)_2$	0.355	4.61±1.13	0.608±0.038
Ph-C-$(OMe)_3$	0.0317	5.97±1.46	0.0764±0.0073
Dendrimer 2.5			
Ph-CH-$(OMe)_2$	0.0164	7.24±6.26	0.0250±0.0060
Ph-C(CH_3)-$(OMe)_2$	0.411	6.39±0.88	0.797±0.041
Ph-C-$(OMe)_3$	0.0365	3.53±0.80	0.0770±0.0060

a) in aqueous 0.1M chloroacetate buffer, pH=3.4, at 25 ± 0.1 °C. k_u values were obtained experimentally, K_S and k_c from fitting of the equation 2 to observed data.

Table 13. Calculated Constants for the Hydrolysis of Carbonyl Carbon Substituted Acetals in Presence of Carboxyl-terminated Dendrimers.

	k_C/k_U	k_2, $M^{-1}s^{-1}$	K_{TS}, mM
Dendrimer 0.5			
Ph-CH-$(OMe)_2$	1.18	7.03	2.51
Ph-C(CH_3)-$(OMe)_2$	1.47	231	1.61
Ph-C-$(OMe)_3$	1.71	6.04	6.19
Dendrimer 1.5			
Ph-CH-$(OMe)_2$	1.35	5.35	2.65
Ph-C(CH_3)-$(OMe)_2$	1.71	132	2.69
Ph-C-$(OMe)_3$	2.41	12.8	2.48
Dendrimer 2.5			
Ph-CH-$(OMe)_2$	1.52	3.45	4.76
Ph-C(CH_3)-$(OMe)_2$	1.94	125	3.30
Ph-C-$(OMe)_3$	2.11	21.8	1.67

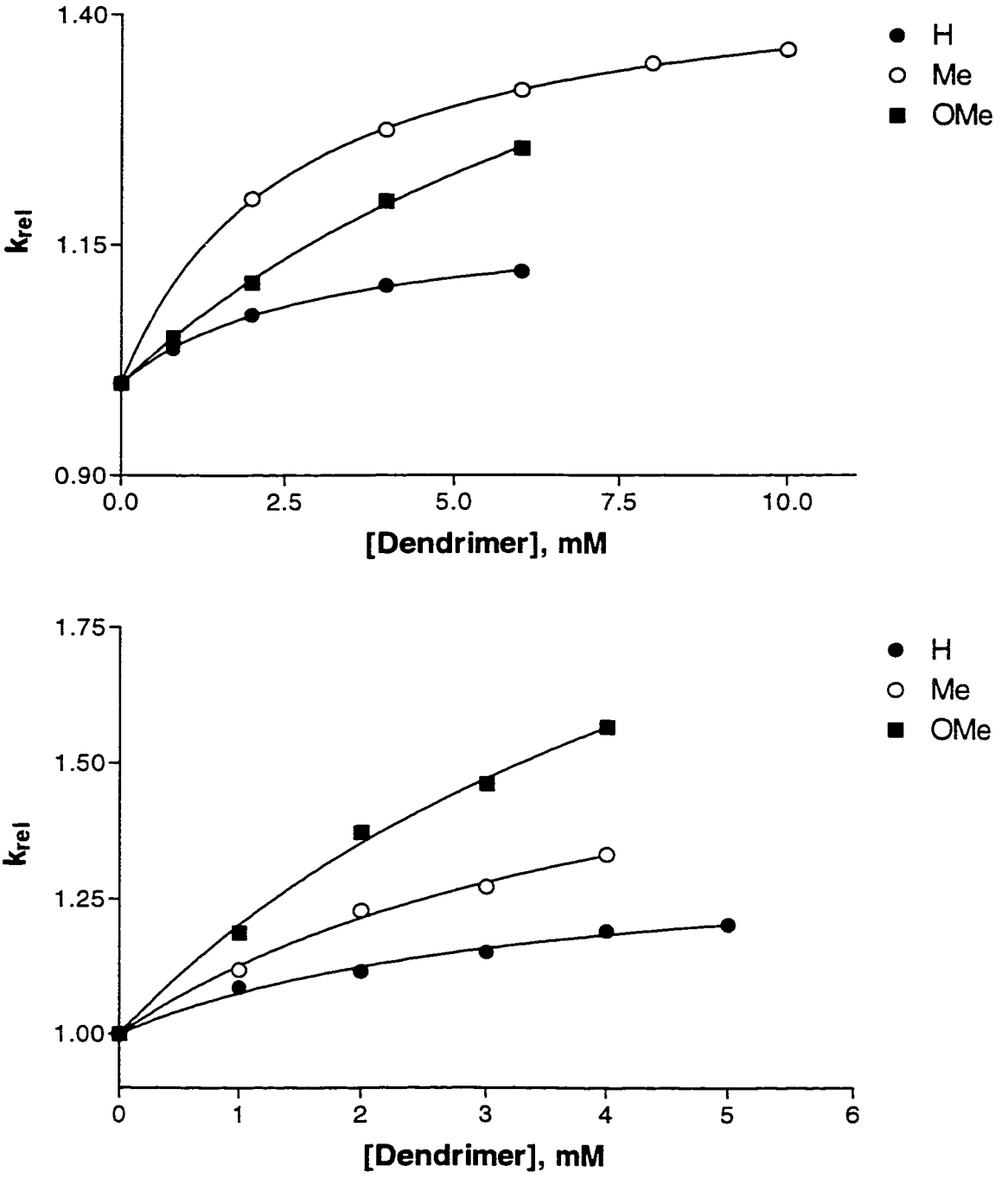

Figure 42. Dependence of Relative Rate Constant for Hydrolysis of Acetals on Dendrimer 0.5 (upper chart) and Dendrimer 1.5 (lower chart) Concentration.

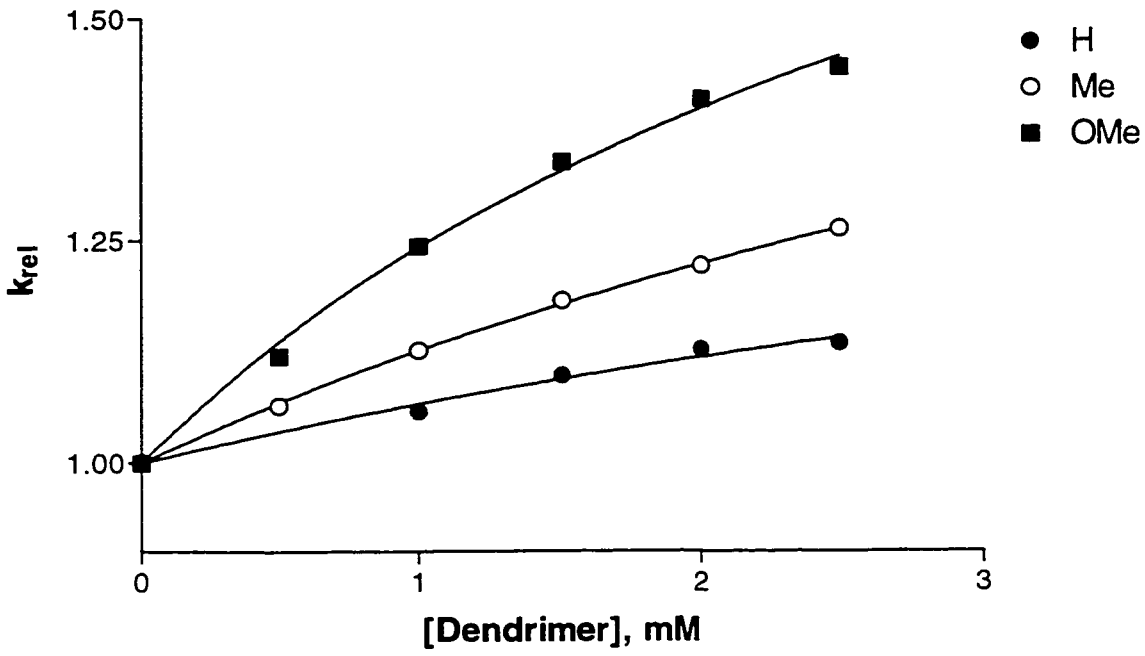

Figure 43. Dependence of Relative Rate Constant for Hydrolysis of Acetals on Dendrimer 2.5 Concentration.

Reactions Mediated by Cyclodextrins.

Cyclodextrins are known to affect the rate of many reactions[5] (see introduction). In recent years in our laboratory we have learned a great deal about cyclodextrin behaviour, their binding properties, and transition state stabilization afforded by these molecules for the variety of reactions[5,11-14,54-56]. However, most of these studies were carried out under the basic conditions. In this section results are presented on the hydrolysis of acetals in presence of different cyclodextrins in acidic solution.

Results and Discussion.

Kinetics studies were made on the cleavage of benzaldehyde dimethyl acetal BDMA), acetophenone dimethyl acetal (ADMA), and trimethyl orthoformate (TMOB) in presence of four different cyclodextrins: α-CD, β-CD, γ-CD, and Hp-β-CD. Raw data are collected in the Appendix 5, and the derived parameters for the reaction which were obtained by fitting of equation 2 to the data are presented in table 14.

All cyclodextrins *decrease* the rate of hydrolysis significantly, exhibiting at the same time saturation kinetics behaviour, *ie.* equation 2, but with $k_c<k_u$ (figures 44, 45, and 46).

Table 14. Constants for the Hydrolysis of Carbonyl Carbon Substituted Acetals in Presence of Cyclodextrins[a,b].

Ester	k_U, s^{-1}	K_S, mM	k_C, s^{-1}	k_C/k_U
α-CD				
Ph-CH-$(OMe)_2$	3.70	46.5	0.588	0.16
Ph-C(CH_3)-$(OMe)_2$	8.00	49.3	3.52	0.44
Ph-C-$(OMe)_3$	8.14	17.3	4.81	0.59
β-CD				
Ph-CH-$(OMe)_2$	3.62	2.26	0	0
Ph-C(CH_3)-$(OMe)_2$	8.02	0.24	0.0507	0.0063
Ph-C-$(OMe)_3$	7.94	0.281	0.573	0.072
Hp-β-CD				
Ph-CH-$(OMe)_2$	3.60	3.64	0	0
Ph-C(CH_3)-$(OMe)_2$	7.86	0.473	0.0284	0.0036
Ph-C-$(OMe)_3$	8.39	0.459	0.216	0.026

(Continued...)

γ-CD				
$Ph\text{-}CH\text{-}(OMe)_2$	3.66	51.3	0	0
$Ph\text{-}C(CH_3)\text{-}(OMe)_2$	7.93	12.6	0.397	0.050
$Ph\text{-}C\text{-}(OMe)_3$	8.12	9.30	0.394	0.049

a) in aqueous 0.1M HCl, at 25 ± 0.1 °C. k_u values were obtained experimentally, K_S and k_c from fitting of the equation 2 to observed data.

b) Following preliminary studies by the author, data for trimethyl orthobenzoate were obtained by Ms. Isabelle Turner, data for acetophenone dimethyl acetal were obtained by Mr. Samer Hussein, and data for the hydrolysis of benzaldehyde dimethyl acetal in presence of γ-CD were obtained by Mr. Patrick Lim Soo.

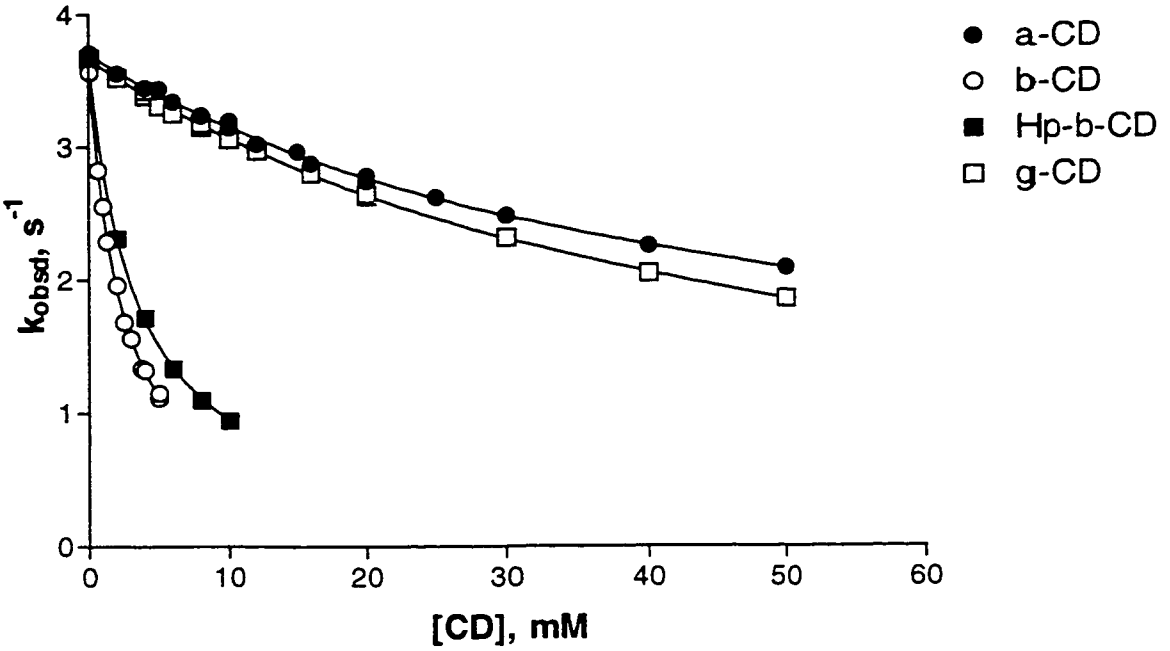

Figure 44. Dependence of Observed Rate Constant k_{obsd} on Cyclodextrin Concentration for the Hydrolysis of Benzaldehyde Dimethyl Acetal.

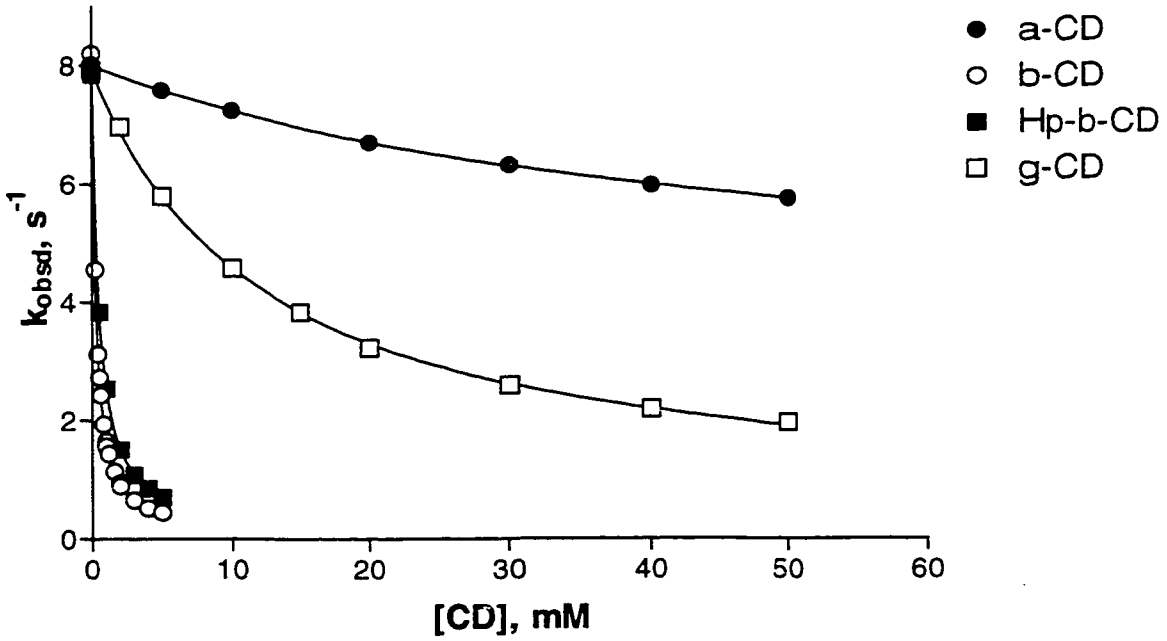

Figure 45. Dependence of Observed Rate Constant k_{obsd} on Cyclodextrin Concentration for the Hydrolysis of Acetophenone Dimethyl Acetal.

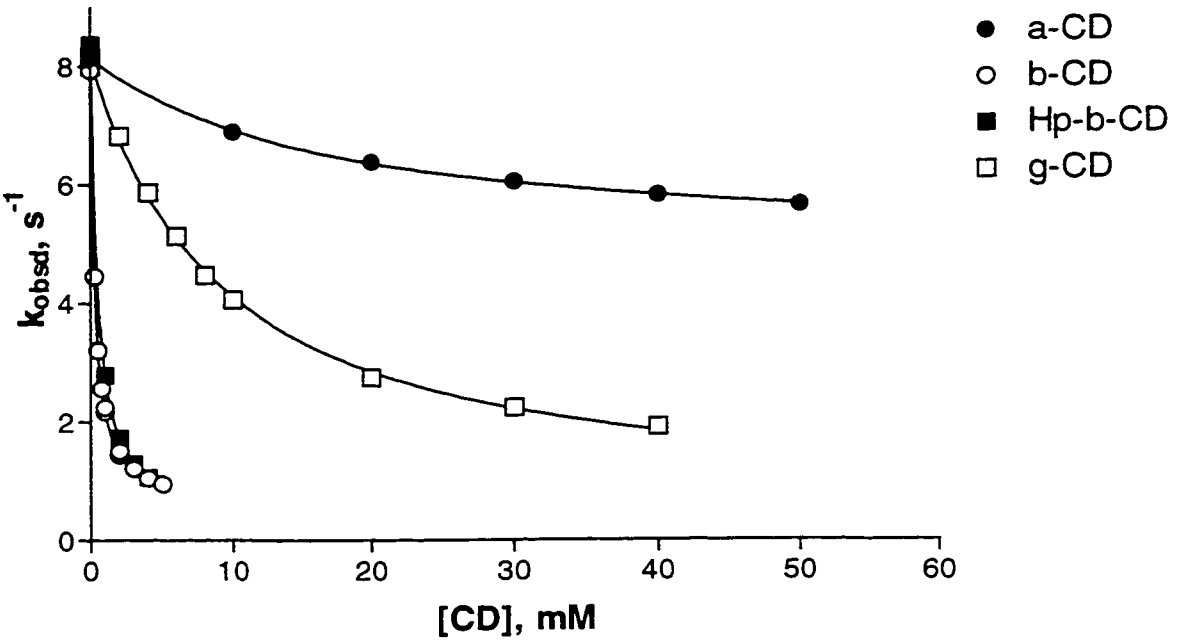

Figure 46. Dependence of Observed Rate Constant k_{obsd} on Cyclodextrin Concentration for the Hydrolysis of Trimethyl Orthobenzoate.

As seen in table 14, the observed substrate binding K_S shows normal tendencies for simple aromatic compounds. For all acetals substrate binding follows the order α-CD<β-CD≈Hp-β-CD>γ-CD. The same order was found for *p*-nitrophenyl alkanoates with short alkyl chains[5], 1- and 2-naphthyl acetates[69] and other derivatives. These results are consistent with relative sizes of cyclodextrin cavities, which follow the same trend. The cavity of α-CD is too small to form a tight complex, and the substrate resides in the upper part of the wider opening of the cyclodextrin. The cavity of γ-CD is too loose, and only β-CD and HP-β-CD provide the best size to form a strong complex (figure 47).

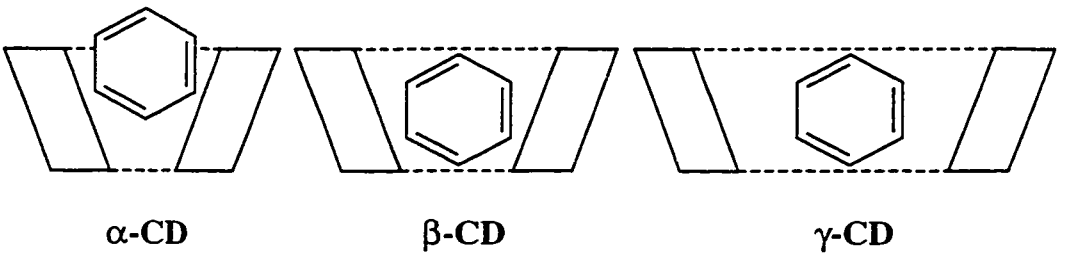

Figure 47. Geometry of Complex Formation for Cyclodextrins with Cavities of Different Sizes.

The influence of the substituent on the carbonyl carbon on the substrate binding can be seen from differences in K_S values of acetals for a given cyclodextrin. Thus the binding of TMOB and ADMA to β-CD, Hp-β-CD, and γ-CD is 5-10 times stronger than binding of BDMA. This is not true, however, in the case of α-CD, which binds BDMA slightly tighter than ADMA. This again can be visualized using scheme in the figure 47: replacing hydrogen with much more bulky

methyl group further prevents the acetal from entering the CD cavity. What may be surprising, is that introducing of even more bulky methoxy group in TMOB results in binding approximately 3 times stronger than with BDMA and ADMA. However, one should keep in mind that wider opening of cavity has secondary hydroxyls, which are capable of donating hydrogen bonds. With the introduction of yet another group which is a hydrogen bond acceptor the CD-acetal complex becomes stronger.

The observed retardation of acetal hydrolysis in presence of cyclodextrins must arise from the TS binding being much less favourable than substrate binding. In other words cyclodextrins actually destabilize the transition state forming in the course of the hydrolysis reaction. The transition state for acetal hydrolysis is believed to be a species lying somewhere between the initially protonated acetal (***a***, figure 48) and carboxonium ion (***b***, figure 48).

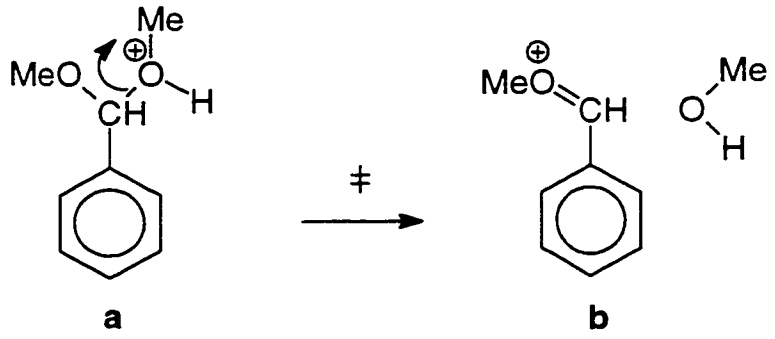

Figure 48. Transition State for Acetal Hydrolysis.

Both structures in the figure 48 have cationic character, but the binding of cations to cyclodextrins has been observed only rarely, and then only for big

molecules like surfactants[48,70].

The suggestion has been made[71] that separation of the newly formed alcohol molecule from the carboxonium ion (structure ***b***, figure 48) might be the rate-limiting step of the reaction of acetal hydrolysis. Cyclodextrins, however, might inhibit this separation, and even favour reaction back to form the initial acetal. Since the overall complex of the structure ***b*** in figure 48 with alcohol molecule also possesses cationic character, both discussed possibilities can operate together to produce the observed inhibition of hydrolysis.

None of the factors discussed above contradict the obtained k_c/k_u values for the acetal hydrolysis. Though inhibition of all the acetals is substantial, BDMA differs from others: with three of the four cyclodextrins hydrolysis is suppressed completely, i.e. the BDMA-cyclodextrin complex is totally unreactive. The only exception is α-CD, and this is understandable, since the geometry of its complex suggests that acetal cannot be completely buried into the cyclodextrin cavity. Electron-donating substituents in ADMA and TMOB partially cancel the factors that disfavour formation of cationic TS, and complete suppression of the hydrolysis in these cases is not observed, although it still very significant.

Other workers in this laboratory have used the CD-inhibited hydrolysis of acetals as kinetic probes of CD-guest binding, using the parameters in table 14. The approach is particularly successful for the binding of guests to β-cyclodextrin and Hp-β-cyclodextrin[72].

Conclusions.

The binding of *p*-nitrophenyl alkanoates to micelles depends on the acyl chain length, and the sensitivity of this parameter on the chain length remains the same regardless the nature of micelles, and therefore, the influence of micelles on the reaction - inhibition or catalysis. However, the magnitude of the rate change is almost independent on the acyl chain length, which is a direct consequence of parallelism between substrate and transition state binding to micelles.

In case of micelles assisted acetal hydrolysis, both substrate binding and magnitude of catalysis are the functions of the substrate structure. Increase of the Hammett reaction constant in the absolute value for the catalysed reaction suggests that transition state develops further, and becomes more sensitive to the electronic effects, exerted by substituents.

Both amino-terminated and carboxylate terminated dendrimers were found to catalyze the cleavage of *p*-nitrophenyl alkanoates, as well as hydrolysis of acetals. The effect of dendrimers on the hydrolysis of acetals, however, is rather small. From the data collected, it is impossible to draw any definite conclusion about processes involved in observed catalysis, though the influence of the internal groups and parts of dendrimers seems to be likely. Experiments on acetal hydrolysis in presence of dendrimers brought another confirmation that interior of PAMAM dendrimers is hydrophilic.

Cyclodextrins are inhibitors of the acidic acetal hydrolysis. This effect results from very unfavourable binding of the transition state to cyclodextrins. Reasons for

that are the fact that transition state of the reaction possesses cationic character, as well as the possibility that cyclodextrins may inhibit diffusional separation of carboxonium ion and methanol, thus promoting the reverse reaction. Among all cyclodextrins, β-CD and Hp-β-CD are much stronger inhibitors of acetal hydrolysis, and this correlates well with the fact, that these two cyclodextrins form stronger complexes with all acetals studied. The strongest complexation was observed in case of benzaldehyde dimethyl acetal, and, as a result, its hydrolysis is suppressed completely when the substrate is saturated with γ-CD, β-CD, or Hp-β-CD.

The inhibited hydrolysis of acetals in the presence of CDs can be used as a probe of CD-guest binding[72].

Experimental.

Most materials (*p*-nitrophenyl alkanoates, benzaldehyde dimethyl acetal, benzaldehyde diethyl acetal, acetophenone dimethyl acetal, trimethyl orthobenzoate, Starburst (PAMAM) dendrimers, sodium dodecyl sulphate (SDS), cetyltrimethylammonium bromide, all buffer components) were purchased from Aldrich Chemical Company. Standard NaOH and HCl solutions were supplied by A & C Chemicals (Montreal). Cetyltrimethylammonium bromide, CTAB, was obtained from ICN Biochemicals, Cleveland. The cyclodextrins were purchased from Aldrich or Wacker-Chemie (Munich, Germany). All chemicals were used as they were supplied.

The substituted benzaldehyde diethyl acetals were synthesized from the corresponding aldehydes using ethanol and triethyl orthoformate, all of which were purchased from Aldrich. For the synthesis, the procedure developed by Fife and Jao[61] was used. Synthesized products were confirmed by ^{1}H NMR analysis, performed on 300 MHz machine Varian Unity Inova 300.

The kinetics were followed using an Applied Photophysics SX17MV Stopped-Flow Spectrophotometer, at a constant temperature of 25±0.1 °C. Absorbance traces that covered 7-10 half-lives were collected from which the first-order rate constant was obtained by non-linear least squares fitting of a first-order exponential to the traces, using software supplied with the spectrophotometer. The wavelength at which each of substrate (or product) was monitored are given in table 15.

Table 15. Monitoring Wavelengths for Compounds used for Kinetic Measurements.

Substrate	Wavelength, nm
p-Nitrophenyl Alkanoates	405
Benzaldehyde dimethyl acetal	252
Acetophenone dimethyl acetal	244
Trimethyl orthobenzoate	237
Benzaldehyde diethyl acetal	243
3-Cl Benzaldehyde diethyl acetal	236
4-Cl Benzaldehyde diethyl acetal	257
4-Bu Benzaldehyde diethyl acetal	252
4-OMe Benzaldehyde diethyl acetal	283

Concentration of *p*-nitrophenyl alkanoate esters were as follows: from pNPA to pNPPent- 50 μM, pNPH- 20 μM, pNPHept- 10 μM, and pNPOct- 5 μM. The concentration of all acetal solutions was 20 μM.

In each case the observed rate constant was taken as an average of 5-15 determinations.

Non-linear fitting of the equations 2 and 15 to data was done with a help of the commercial statistical package Prism™, produced by GraphPad Corporation

(San Diego, USA).

List of References.

1. Philp, D., Stoddart, J.F., *Angew. Chem., Int. Ed. Engl.*, **35**, 1154, 1996.
2. Vögtle, F., *Supramolecular Chemistry*, John Wiley and Sons, NY, 1991.
3. *Frontiers in Supramolecular Organic Chemistry and Photochemistry* (Schneider, H.J., Dürr, H, eds.), VCH, NY, 1991.
4. Tomalia, D.A., *Aldrichimica Acta*, **26**, 91, 1993.
5. Tee, O.S., *Adv. Phys. Org. Chem.*, **29**, 1, 1993.
6. Gadosy, T.A., *Ph.D. Thesis*, Concordia University, 1995.
7. Tee, O.S, Mazza, C., Lozano-Hemmer., R., Giorgi, J.B., *J. Org. Chem.*, **59**, 7602, 1994.
8. Tee, O.S., Giorgi, J.B., *J. Amer. Chem. Soc.*, **117**, 3633, 1995.
9. Rosen, M.J., *Surfactants and Interfacial Phenomena*, John Wiley and Sons, NY, 1989.
10. Fendler, J.H., Fendler, E.J., *Catalysis in Micellar and Macromolecular Systems*, Academic Press, NY, 1975.
11. Tanford, C., *The Hydrophobic Effect: Formation of Micelles and Biological Membranes*, John Wiley and Sons, NY, 1980.
12. Moroi, Y., *Micelles: Theoretical and Applied Aspects*, Plenum Press, NY, 1992.
13. Menger, F.M., in *Surfactants in Solution* (Mittal, K.L., Lindman, B. eds), v.1, 347, Plenum Press, NY, 1984.

14. Menger, F.M., *Acc. Chem. Res.*, **12**, 111, 1979.

15. Bunton, C.A., Savelli, G., *Adv. Phys. Org. Chem.*, **22**, 213, 1986.

16. Dunlap, B.R., Cordes, E.H., *J. Amer. Chem. Soc.*, **90**, 4395, 1968.

17. Menger, F.M., Portnoy, C.E., *J. Amer. Chem. Soc.*, **89**, 4698, 1967.

18. Behme, M.T.A., Fullington, J.G., Noel, R., Cordes, E.H., *J. Amer. Chem. Soc.*, **87**, 266, 1965.

19. Romsted, L.R., Cordes, E.H., *J. Amer. Chem. Soc.*, **90**, 4404, 1968.

20. Dunlap, B.R., Ghanim, G.A., Cordes, E.H., *J. Phys. Chem.*, **73**, 1898, 1969

21. Dunlap, B.R., Cordes, E.H., *J. Phys. Chem.*, **73**, 361, 1969.

22. Cerichelli, G., Grande, C., Luchetti, L., Mancini, G., *J. Org. Chem.*, **52**, 5167, 1987.

23. Bunton, C.A., Robinson, L., *J. Phys. Chem.*, **73**, 4237, 1969.

24. Cordes, E.H., Dunlap, B.R., *Acc. Chem. Res.*, **2**, 329, 1969.

25. *Reaction Kinetics in Micelles* (Cordes, E.H. ed.), Plenum Press, NY, 1973.

26. Quina, F.H., Politi, M.J., Cuccovia, I.M., Martins-Franchetti, S.M., Chaimovich, H., in *Surfactants in Solution* (Mittal, K.L., Lindman, B. eds), v.2, 1125, Plenum Press, NY, 1984.

27. Herries, D.G., Bishop, W., Richards, F.M., *J. Phys. Chem.*, **68**, 1842, 1964.

28. Al-Awadi, N., Williams, A., *J. Org. Chem.*, **55**, 2001, 1990.

29. Romsted, L.S., *in Surfactants in Solution* (Mittal, K.L., Lindman, B. eds), v.2, 1015, Plenum Press, NY, 1984.

30. Romsted, L.S., in *Micellization, Solubilization, and Microemulsions* (Mittal,

K.L., ed.), v.2, 509, 1977.

31. Quina, F.H., Chaimovich, H., *J. Phys. Chem.*, **83**, 1844, 1979.

32. Flory, P.J., *J. Amer. Chem. Soc.*, **63**, 3083, 1941.

33. Flory, P.J., *J. Phys. Chem.*, **17**, 303, 1949.

34. Newkome, G.R., Moorefield, C.N., Vögtle, F., *Dendritic Molecules*, VCH, NY, 1996.

35. Newkome, G.R., Moorefield, C.N., Baker, G.R., *Aldrichimica Acta*, **25**, 31, 1992.

36. Stevelmans, S., van Hest, J.C.M., Jansen, J.F.G.A., van Boxtel, D.A.F.J., de Brabander-van den Berg, E.M.M., Meijer, E.W., *J. Amer. Chem. Soc.*, **118**, 7398, 1996.

37. Tomalia, D.A., Naylor, A.M., Goddard III, W.A., *Angew. Chem. Int. Ed. Engl.*, **29**, 138, 1990.

38. Gopidas, K.R., Leheny, A.R., Caminati, G., Turro, N.J., Tomalia, D.A., *J. Amer. Chem. Soc.*, **113**, 7335, 1991.

39. Caminati, G., Turro, N.J., Tomalia, D.A., *J. Amer. Chem. Soc.*, **112**, 8515, 1990.

40. Ottaviani, F.M., Bossmann, S., Turro, N.J., Tomalia, D.A., *J. Amer. Chem. Soc.*, **116**, 661, 1994.

41. Jansen, J.F.G.A., de Brabander-van den Berg, E.M.M., Meijer, E.W., Science, **266**, 1226, 1994.

42. *Industrial Applications of Starburst Polyamidoamine (PAMAM) Dendrimers,*

Technology Review, Dendritech, Inc., Sec.9, 9.2, 1995.

43. Bender, M.L., Komiyama M. *Cyclodextrin Chemistry*, Springer-Verlag, 1978.

44. Szejtli, J. *Cyclodextrins and Their Inclusion Complexes*, Akademia Kiado, Budapest, 1982.

45. Szejtli, J. *Inclusion Compounds,* vol. 3, Chapter 11, Academic Press, London, 1984.

46. Lindoy, L.F. *The Chemistry of Macrocyclic Ligands*, Cambridge University Press, 1989.

47. Hyble, A., Rundle, R.E., Williams, D.E. *J. Am. Chem. Soc.,* **87**, 2779, 1965.

48. French, D., Rundle, R.E. *J. Am. Chem. Soc.,* **64**, 1651, 1942.

49. Wojcik, J.F., Rohrbach, R.P. *J. Phys. Chem.*, **79**, 2251, 1975.

50. Cramer, F., Henglein, F.M. *Angew. Chem.*, **68**, 649, 1956.

51. VanEtten, R.L., Sebastian, J.F., Clowes, G.A., Bender, M.L. *J. Am. Chem. Soc.,* **89**, 3242, 1967.

52. Park, J.W., Song H.J. *J. Phys. Chem.,* **93**, 6454, 1989.

53. Cramer, F., Saenger, W., Spatz, H-Ch. *J. Am. Chem. Soc.*, **89**, 14, 1967.

54. Tee, O.S., Mazza, C., Du, X-X. *J. Org. Chem.*, **55**, 3603, 1990.

55. Tee, O.S., Gadosy, T.A., Giorgi, J.B. *J. Chem. Soc., Perkin Trans. 2,* 1705, 1993.

56. Tee, O.S., Gadosy, T.A., Giorgi, J.B. *Can. J. Chem.*, **74**, 736,1996.

57. Straub, T.S., Bender, M.L. *J. Am. Chem. Soc.,* **94**, 8881, 1972.

58. Straub, T.S., Bender, M.L. *J. Am. Chem. Soc.,* **94**, 8875, 1972.

59. Jencks, W.P., *Chem. Rev.*, **72**, 705, 1972.

60. Bull, H.G., Cordes, E.H., *Chem. Rev.*, **74**, 581, 1974.

61. Fife, T.H., Jao, L.K., *J. Org. Chem.*, **30**, 1492, 1964.

62. Jensen, J.L., Wuhrman, W.B., *J. Org. Chem.*, **48**, 4686, 1983.

63. Jensen, J.L., Herold, L.R., Lenz, P.A., Trusty, S., Sergi, V., Bell, K., Rogers, P., *J. Amer. Chem. Soc.*, **101**, 4672, 1979.

64. McClelland, R.A., Sörensen, P., *Acta Chem. Scand.*, **44**, 1082, 1990.

65. Kurz, J.L., *J. Amer. Chem. Soc.*, **85**, 987, 1963.

66. Laidler, K.J., *Chemical Kinetics*, 3 ed., Harper & Row, NY, 1987.

67. Sykes, P., *A Guidebook to Mechanism in Organic Chemistry*, 6 ed., John Wiley & Sons, NY, 1986.

68. Evans, D.J., Kanagasooriam, A., Williams, A., *J. Mol. Cat.*, **85**, 21, 1993.

69. Tee, O.S., Boyd, M.J., *J. Chem. Soc., Perk. Trans. 2*, 1237, 1995.

70. Okubo, T., Kitano, H., Ise, N., *J. Phys. Chem.*, **80**, 2661, 1976.

71. Jensen, J.L., Yamaguchi, K.S., *J. Org. Chem.*, **49**, 2613, 1984.

72. a) Tee, O.S., Fedortchenko. A.A., Lim Soo, P., *J. Chem. Soc., Perk. Trans. 2*, in press;

b) Turner, I., studies in progress;

c) Hussein, S., studies in progress.

Appendix I.

Table A1.1. Raw Data for the Cleavage of *p*-Nitrophenyl Alkanoates in Presence of CTAB.

	k_{obsd}, s^{-1}		
[CTAB], mM	C_2	C_3	C_4
0	0.1102	0.1067	0.0693
0.5	0.1180	0.1176	0.0868
1	0.1251	0.1270	0.1010
2	0.1390	0.1422	0.1165
3	0.1501	0.1540	0.1245
4	0.1598	0.1621	0.1308
5	0.1682	0.1694	0.1354

	k_{obsd}, s^{-1}			
[CTAB], mM	C_5	C_6	C_7	C_8
0	0.0697	0.0649	0.0630	0.0591
0.5	0.1051	0.1265	0.1478	0.1399
0.75	0.1146	0.1362	0.1522	0.1411
1	0.1210	0.1416	0.1537	0.1435
2	0.1355	0.1501	0.1577	
3	0.1410	0.1534	0.1588	
4	0.1456	0.1539	0.1597	
5	0.1486	0.1542	0.1603	

Table A1.2. Raw Data for the Cleavage of *p*-Nitrophenyl Alkanoates in Presence of SDS.

	k_{obsd}, s^{-1}		
[SDS], mM	C_2	C_3	C_4
0	0.104	0.0996	0.0649
4	0.0899	0.0739	0.0337
8	0.0767	0.0561	0.0208
12	0.0697	0.0449	0.0156
16	0.0596	0.0358	0.0124
20	0.0537	0.0308	0.0104

	k_{obsd}, s^{-1}	
[SDS], mM	C_5	C_6
0	0.0653	0.0532
4	0.0194	0.00829
8	0.0102	0.00395
12	0.00669	0.00265
16	0.00535	0.00189
20	0.00437	0.00173

Appendix II.

Table A2.1. Raw Data for the Hydrolysis of Acetals in Presence of SDS.

	k_{obsd}, s^{-1}			
[SDS], mM	TMOB	BDMA	4-Bu BDEA	ADMA
0	0.0395	0.0157	0.191	0.421
1				0.431
2	0.0873	0.0190	3.33	0.671
4	0.245	0.0314	4.33	1.60
8	0.439	0.0517	4.51	2.88
12	0.554	0.0672	4.64	3.76
16	0.617	0.0788	4.67	4.34
20	0.659	0.0873		4.70

	k_{obsd}, s^{-1}			
[SDS], mM	BDEA	4-OMe-BDEA	3-Cl-BDEA	4-Cl-BDEA
0	0.0528	0.666	0.00414	0.0189
2	0.0974	3.18	0.0103	0.0503
4	0.205	8.61	0.0181	0.0950
8	0.338	15.0	0.0227	0.123
12	0.404	18.3	0.0237	0.132
16	0.444	19.9	0.0239	0.136
20	0.464	20.8	0.0241	0.131

Appendix III.

Table A3.1. Raw Data for the Cleavage of *p*-Nitrophenyl Alkanoates in Presence of Dendrimer 0.

	k_{obsd}, s^{-1}		
[Dendrimer 0], mM	C_2	C_3	C_4
0	0.0651	0.0649	0.0407
2	0.0885	0.0840	0.0527
4	0.110	0.102	0.0622
6	0.131	0.119	0.0730
8	0.150	0.135	
10	0.166	0.150	0.0905

	k_{obsd}, s^{-1}			
[Dendrimer 0], mM	C_5	C_6	C_7	C_8
0	0.0418	0.0376	0.0394	0.0358
2	0.0559	0.0498	0.0514	0.0489
4	0.0673	0.0608	0.0618	0.0602
6	0.0791	0.0713	0.0715	0.0691
8	0.0903	0.0792	0.0800	0.0787
10	0.100	0.0893	0.0875	

Table A3.2. Raw Data for the Cleavage of *p*-Nitrophenyl Alkanoates in Presence of Dendrimer 1.

	k_{obsd}, s^{-1}		
[Dendrimer 1], mM	C_2	C_3	C_4
0	0.0861	0.0914	0.0577
1	0.119	0.124	0.0790
2	0.151	0.156	0.0998
4	0.212	0.212	0.123
6	0.264	0.256	0.150
8	0.308	0.294	0.173
9	0.325	0.313	0.180
10	0.343	0.324	0.189

	k_{obsd}, s^{-1}	
[Dendrimer 1], mM	C_5	C_6
0	0.0464	0.0449
0.5	0.0650	0.0626
1	0.0830	0.0809
1.5	0.119	0.112
2	0.151	0.142
3	0.179	0.174
4	0.194	0.185
5	0.205	0.196

	k_{obsd}, s^{-1}	
[Dendrimer 1], mM	C_7	C_8
0	0.0481	0.0468
1.91	0.0860	0.0771
3.82	0.104	0.105
5.73	0.128	0.124
7.64	0.148	0.143
9.55	0.164	0.152

Table A3.3. Raw Data for the Cleavage of *p*-Nitrophenyl Alkanoates in Presence of Dendrimer 2.

	k_{obsd}, s^{-1}	
[Dendrimer 2], mM	C_2	C_3
0	0.0999	0.0973
0.96	0.0189	
1.93	0.269	0.204
2.89	0.340	0.249
3.85	0.405	0.293
4.81	0.459	0.323

	k_{obsd}, s^{-1}	
[Dendrimer 2], mM	C_4	C_6
0	0.0428	0.0354
0.8	0.0749	0.0709
1.6	0.105	0.0988
2.4	0.136	0.120
3.2	0.155	0.134
4	0.174	0.154

[Dendrimer 2], mM	k_{obsd}, s^{-1}		
	C_5	C_7	C_8
0	0.0436	0.0364	0.0352
1	0.0834	0.0721	0.0703
2	0.116	0.102	0.0950
3	0.137	0.130	0.115
4	0.156	0.142	0.130
5	0.174	0.151	0.136

Table A3.4. Raw Data for the Cleavage of *p*-Nitrophenyl Alkanoates in Presence of Dendrimer 3.

	k_{obsd}, s^{-1}		
[Dendrimer 3], mM	C_2	C_3	C_4
0	0.0741	0.0650	0.0417
0.5	0.165	0.125	0.0803
1	0.241	0.177	0.113
1.5	0.304	0.218	0.138
2.5	0.399	0.270	0.169

	k_{obsd}, s^{-1}			
[Dendrimer 3], mM	C_5	C_6	C_7	C_8
0	0.0409	0.0391	0.0445	0.0461
0.5	0.0827	0.0799	0.0823	0.0827
1	0.117	0.102	0.112	0.0979
1.5	0.142	0.123	0.133	0.110
2.5	0.173	0.149	0.155	0.119

Table A3.5. Raw Data for the Cleavage of *p*-Nitrophenyl Alkanoates in Presence of Dendrimer 0.5.

pH=11.6	k_{obsd}, s^{-1}		
[Dendrimer 0.5], mM	C_2	C_4	C_6
0.00	0.0701	0.0427	0.0407
2.00	0.101	0.0614	0.0611
4.00	0.132	0.0793	0.0787
6.00	0.161	0.0965	0.0955
8.00	0.189	0.111	0.111
10.00	0.217	0.125	0.126

pH=10.6	k_{obsd}, s^{-1}		
[Dendrimer 0.5], mM	C_2	C_4	C_6
0.00	0.00818	0.00490	0.00643
2.00	0.0107	0.00615	0.00912
4.00	0.0131	0.00757	0.0111
6.00	0.0150	0.00839	0.0125
8.00	0.0167	0.00942	0.0135
10.00	0.0180	0.0100	0.0144

Table A3.6. Raw Data for the Cleavage of *p*-Nitrophenyl Alkanoates in Presence of Dendrimer 1.5.

pH=11.6	k_{obsd}, s^{-1}		
[Dendrimer 1.5], mM	C_2	C_4	C_6
0	0.0635	0.0382	0.0374
1	0.0955	0.0568	0.0545
2	0.121	0.0729	0.0704
3	0.141	0.0853	0.0891
4	0.173	0.100	0.101
5	0.194	0.109	0.110

pH=10.6	k_{obsd}, s^{-1}		
[Dendrimer 1.5], mM	C_2[a]	C_4	C_6
0	0.00789	0.00305	0.00290
0.5	0.0106	0.00370	0.00365
0.9	0.0127	0.00409	0.00396
1.8	0.0144	0.00499	0.00458
3.6	0.0158	0.00603	0.00564
5	0.0176	0.00646	0.00600

a) the range of concentrations for C_2 at pH=10.6 is: 0,1,2,3,4,5 mM

Table A3.7. Raw Data for the Cleavge of *p*-Nitrophenyl Alkanoates in Presence of Dendrimer 2.5.

pH=11.6	k_{obsd}, s^{-1}		
[Dendrimer 2.5], mM	C_2	C_4	C_6
0	0.101	0.0630	0.0612
0.5	0.147	0.0901	0.0841
1	0.191	0.116	0.109
1.5	0.232	0.139	0.131
2	0.265	0.155	0.150
2.5	0.292		0.165

pH=10.6	k_{obsd}, s^{-1}		
[Dendrimer 2.5], mM	C_2	C_4	C_6
0.00	0.0105	0.00625	0.00556
0.25	0.0126	0.00736	0.00710
0.5	0.0141	0.00811	0.00786
0.9	0.0167	0.00945	0.00901
1.8	0.0212	0.0119	0.0110
2.50	0.0244	0.0124	0.0117

Appendix IV.

Table A4.1. Raw Data for the Hydrolysis of Acetals in Presence of Dendrimer 0.5.

	k_{obsd}, s^{-1}		
[Dendrimer 0.5], mM	BDMA	ADMA	TMOB
0	0.0176	0.377	0.0373
0.8	0.0183		0.0392
2	0.0189	0.452	0.0414
4	0.0195	0.480	0.0447
6	0.0198	0.496	0.0469
8		0.507	
10		0.513	

Table A4.2. Raw Data for the Hydrolysis of Acetals in Presence of Dendrimer 1.5.

	k_{obsd}, s^{-1}		
[Dendrimer 1.5], mM	BDMA	ADMA	TMOB
0	0.0141	0.355	0.0317
1	0.0154	0.397	0.0376
2	0.0158	0.436	0.0435
3	0.0163	0.451	0.0463
4	0.0168	0.473	0.0496
5	0.0170		

Table A4.3. Raw Data for the Hydrolysis of Acetals in Presence of Dendrimer 2.5.

	k_{obsd}, s^{-1}		
[Dendrimer 2.5], mM	BDMA	ADMA	TMOB
0	0.0164	0.411	0.0365
0.5	0.0167	0.438	0.0408
1	0.0173	0.463	0.0454
1.5	0.0180	0.486	0.0488
2	0.0185	0.502	0.0514
2.5	0.0186	0.519	0.0527

Appendix V.

Table A5.1. Raw Data for the Hydrolysis of TMOB in Presence of Cyclodextrins.

	k_{obsd}, s^{-1}			
[CD], mM	α-CD	β-CD	Hp-β-CD	γ-CD
0				8.17
0	8.14	7.93	8.38	8.01
0.25		4.45		
0.5		3.21		
0.75		2.56		
1		2.17	2.79	
1		2.25		
2		1.44	1.73	6.82
2		1.50		
3		1.21	1.29	
4		1.05	1.06	5.87
5		0.95		
6				5.14
8				4.48
10	6.89			4.06
20	6.38			2.75
30	6.05			2.24

(Continued ...)

40	5.81			1.91
50	5.64			

Table A5.2. Raw Data for the Hydrolysis of BDMA in Presence of Cyclodextrins.

	k_{obsd}, s^{-1}			
[CD], mM	α-CD	β-CD	Hp-β-CD	γ-CD
0.0	3.70	3.67	3.60	3.66
0.0	3.69	3.56		3.67
0.0	3.70			3.67
0.625		2.83		
1.0		2.55		
1.25		2.29		
2.0	3.56	1.96	2.31	3.52
2.5		1.69		
3.0		1.56		
3.75		1.34		
4.0	3.44	1.32	1.72	3.39
4.0	3.44			3.42
5.0		1.11		3.31
5.0	3.44	1.15		
6.0	3.34		1.34	3.25

(Continued ...)

8.0	3.23	1.10	3.15
8.0	3.23		3.18
10.0	3.13	0.946	3.06
10.0	3.19		3.06
12.0	3.02		2.97
15.0	2.96		
16.0	2.87		2.80
20.0	2.74		2.63
20.0	2.78		2.64
25.0	2.62		
30.0	2.48		2.32
40.0	2.25		2.05
50.0	2.09		1.86

Table A5.3. Raw Data for the Hydrolysis of ADMA in Presence of Cyclodextrins.

	k_{obsd}, s^{-1}			
[CD], mM	α-CD	β-CD	Hp-β-CD	γ-CD
0	8.00	8.20	7.86	7.93
0		8.01		
0.2		4.55		
0.4		3.13		

(Continued ...)

0.5		2.73	3.84	
0.6		2.43		
0.8		1.94		
1		1.65	2.54	
1		1.57		
1.2		1.44		
1.6		1.14		
2		0.944	1.51	6.98
2		0.897		
3		0.661	1.09	
4		0.525	0.864	
5	7.59	0.454	0.712	5.80
10	7.23			4.58
15				3.84
20	6.70			3.23
30	6.32			2.60
40	5.98			2.20
50	5.75			1.96

0.5		2.73	3.84	
0.6		2.43		
0.8		1.94		
1		1.65	2.54	
1		1.57		
1.2		1.44		
1.6		1.14		
2		0.944	1.51	6.98
2		0.897		
3		0.661	1.09	
4		0.525	0.864	
5	7.59	0.454	0.712	5.80
10	7.23			4.58
15				3.84
20	6.70			3.23
30	6.32			2.60
40	5.98			2.20
50	5.75			1.96